Energy, Ecology and Environment
https://doi.org/10.1007/s40974-024-00338-4

CORRESPONDENCE

A new method for simulation-based sensitivity analysis of building efficiency for optimal building energy planning: a case study of Iran

Masoud Nasouri[1] · **Navid Delgarm**[2]

[1] Department of Environment, University of Tehran, Aras International Campus, P.O. Box 1417763133, Tehran, Iran
[2] Department of Mechanical Engineering, College of Engineering, University of Tehran, P.O. Box 1417935840, Tehran, Iran

Received: 2 December 2023 / Revised: 23 July 2024 / Accepted: 14 August 2024

Abstract This work provides a Simulation-Based Sensitivity Analysis (SBSA) framework for optimal building energy planning during the conceptual design phase. The innovative approach integrates EnergyPlus with local sensitivity analysis (LSA) and global sensitivity analysis (GSA) algorithms, thereby facilitating direct sensitivity analysis (SA) capabilities without reliance on external plugins or third-party tools. The effectiveness of this approach is exemplified through its application to a residential building situated in a hot semi-arid climate region of Iran. The efficacy of the developed approach is demonstrated by applying it to a residential building located in a hot semi-arid climate region in Iran. The study utilizes four primary building performance criteria as output variables: annual heating energy consumption (AHC), annual cooling energy consumption (ACC), annual lighting energy consumption (ALC), and the predicted percentage of dissatisfied (PPD). The study employs one-at-a-time (OAT) analysis for LSA and Sobol's analysis for GSA to investigate the behavior of output variables in response to changes in building design parameters. In the LSA approach, a newly developed sensitivity indicator, termed the Dispersion Index (DI), is introduced to precisely measure the overall sensitivity of outputs to inputs (S_T). Results indicate that annual AHC is most sensitive to the heating setpoint (S_T = 80%) and solar absorptance of exterior walls (S_T = 79%), while annual cooling consumption (ACC) is primarily influenced by the cooling setpoint (S_T = 72%) and solar absorptance of exterior walls (S_T = 63%). Additionally, window-to-wall ratio (WWR), visible transmittance of window glass, and building rotation significantly affect annual lighting consumption (ALC) (S_T = 33%, 25%, and 21% respectively). Furthermore, cooling and heating setpoints, solar absorptance of exterior walls, and WWR play crucial roles in PPD (S_T = 81%, 40%, 36%, and 21% respectively). Notably, ALC shows no dependence on variable air volume (VAV) setpoint temperatures and thermophysical properties of walls and windows. Besides, the proposed DI in OAT-based LSA shows strong alignment with the results achieved by the Sobol-based GSA. This systematic approach, termed SBSA, empowers building designers and decision-makers to pinpoint critical design parameters early in the conceptual phase, ensuring optimal building performance. The flexibility of the SBSA framework accommodates diverse building configurations, facilitating comprehensive SA without constraints.

Keywords Sensitivity analysis · Integration framework · OAT analysis · Sobol's analysis · Building performance

Abbreviations

ACC	Annual cooling energy consumption
AHC	Annual heating energy consumption
ALC	Annual lighting energy consumption
ATC	Annual total energy consumption
BF	Building facade
BPA	Building performance analysis
BR	Building rotation
BTO	Building technologies office
CDD	Cooling degree-day
CTSP	Cooling setpoint temperature
DI	Dispersion index
DOE	Department of energy

✉ Navid Delgarm
navid.delgarm@ut.ac.ir

Masoud Nasouri
M.Nasouri@ut.ac.ir

Published online: 17 September 2024

GSA	Global sensitivity analysis
HDD	Heating degree-day
HTSP	Heating setpoint temperature
HVAC	Heating, ventilation, and air conditioning
LSA	Local sensitivity analysis
MIP	Mixed-integer programming
OAT	One-at-a-time
PCM	Phase change material
PMV	Predicted mean vote
PPD	Predicted percentage of dissatisfied
SA	Sensitivity analysis
SALib	Sensitivity analysis library
DSH	Depth of shading device
SI	Sensitivity index
SBSA	Simulation-based sensitivity analysis
VAV	Variable air volume
WWR	Window-to-wall ratio

List of symbols

SA_{Ex_W}	Solar absorptance of the exterior wall
SA_{IN_W}	Solar absorptance of the interior wall
S_T	Total-order sensitivity index
ST_{win}	Solar transmittance of window glass
Th_{Ex_W}	Thickness of wall
$Th_{gas-win}$	Thickness of gas in window
Th_{win}	Thickness of window glass
VT_{win}	Visible transmittance of window glass

1 Introduction

The continuous combustion of fossil fuels releases a multitude of environmental pollutants, severely damaging both ecosystems and public health, and highlights the urgent need for renewable energy sources (Ramin et al. 2015; Nasouri and Delgarm 2022a, b). In the meantime, the building industry accounts for 31% of the world's total energy use and 27% of energy-related global emissions (Zamanipour et al. 2023). In Iran, buildings consume 41% of the nation's total energy and contribute 36% of its CO_2 emissions (Delgarm et al. 2018), with energy consumption in this sector being 3 to 5 times the global average and twice the international rate (Delgarm et al. 2016b; Lotfabadi and Hançer 2023). Forecasted population growth will likely increase energy demand in Iran's building sector, further compounded by its substantial dependence on fossil fuels, thus intensifying the environmental crisis (Delgarm et al. 2016c). Alongside energy efficiency, ensuring the comfort of occupants is crucial in building design (Zheng et al. 2022; Wang et al. 2023). Occupants' thermal comfort is a state of mind that indicates satisfaction with the thermal conditions of the environment (ANSI/ASHRAE Standard 55 2010). Among the well-known thermal comfort models, the predicted mean vote (PMV) and predicted percentage of dissatisfied (PPD) models are the most widely used (Charai et al. 2022; Almagro-Lidón et al. 2024), initially expressed by Fanger (Fanger 1970). The PMV model estimates the average thermal sensation of a large group of individuals using a seven-point scale, ranging from + 3 (hot) to − 3 (cold) (Salilih et al. 2022). Adding that, PPD model provides a numerical forecast of the proportion of people likely to be thermally uncomfortable, as inferred from the PMV scores. ANSI/ASHRAE 55 recommends maintaining PPD under 10% and PMV between − 0.5 and + 0.5 for general comfort.

Achieving energy efficiency in buildings becomes viable when it aligns with the thermal comfort requirements of occupants. During the early stages of building design, decision-makers face the challenge of navigating through complex, multivariate problems inherent in construction projects (Salilih et al. 2022). This process involves evaluating numerous feasible combinations of building specifications to determine optimal design choices (Kayalica et al. 2020). Neglecting design principles during the early stages may lead to erroneous selection of building materials and equipment, resulting in poor building performance. Therefore, achieving optimal building performance necessitates meticulous consideration and adoption of the most suitable design parameters.

Building designers employ various building simulation tools, including EnergyPlus, TRACE, Carrier HAP, DesignBuilder, eQUEST, and TRNSYS, to evaluate and forecast building performance (Delgarm et al. 2016c; Hollberg et al. 2017; Essa 2021; Arfi et al. 2023). These tools typically execute building models on a scenario-by-scenario basis, a process known for its significant time consumption and impracticality in assessing all potential cases comprehensively. Often, this approach yields unreasonable and imprecise results due to the limited number of scenarios evaluated relative to the full range of possible scenarios (Shin and Haberl 2022; Nasouri and Delgarm 2023). Therefore, to address this challenge, integrating building simulation software with sensitivity analysis (SA) algorithms allows for investigating the attribution of output uncertainties to various inputs, identifying technical simulation errors, pinpointing sensitive and critical parameters, prioritizing areas for improvement, simplifying models, detecting analysis inaccuracies, and offering valuable insights for optimization purposes (Dara and Hachem-Vermette 2019; Carpino et al. 2022). There are numerous methods available for conducting sensitivity analysis (SA) on systems, typically categorized into two main types: local sensitivity analysis (LSA) and global sensitivity analysis (GSA) (Mendes et al. 2022; Li et al. 2023). LSA focuses on assessing the local impact of input variations on

the system's response (Rentzeperis and Wallace 2022; Hai et al. 2022). The one-at-a-time (OAT) is a well-established technique in LSA (Nasouri et al. 2021, 2022a, b). It involves assessing the impact of individual parameters on the outputs while maintaining all other system parameters at their nominal (baseline) values. This method systematically evaluates each parameter sequentially, repeating the process for each parameter in a similar manner (Falk et al. 2021; Saha et al. 2023). In this context, the SA quantifies the impact of individual parameter variations within their specified ranges on output variables. While the OAT is straightforward to apply and efficient in terms of computational time, it overlooks the combined effects and interactions among inputs on outputs. Consequently, it may yield misleading results regarding the prioritization of design parameters based on their influence on the system, particularly in nonlinear and complex models like building systems. In contrast, GSA involves simultaneously varying all input parameters within their respective ranges to evaluate system sensitivity (Xu et al. 2023). This approach considers the interactions and mutual influences among inputs, providing a more accurate assessment of how each input affects the system compared to LSA (Vuillod et al. 2023). Nevertheless, GSA methods generally require significantly more computation time compared to LSA methods, especially when dealing with complex models that involve a large number of input parameters (Liu et al. (2023). Various techniques have been proposed for conducting GSA in the context of buildings, encompassing regression-based, Morris method, variance-based, and metamodeling-based approaches (Zhang et al. 2020). Among these, variance-based methods have garnered significant attention and adoption (Pianosi and Wagener 2015; Kala 2021; Belyamin et al. 2021). Sobol's method (Saltelli et al. 2007) is renowned as a prominent variance-based GSA approach widely utilized for complex non-linear models (Lo Piano et al. 2021). This method adeptly captures intricate interactions among inputs through advanced sampling methodologies to accurately assess sensitivity indicators (Zhang et al. 2015).

Over the past decade, the focus of numerous researchers and decision-makers has shifted towards SA of building performance, owing to its provision of valuable insights during the initial stages of building design. Pang et al. (2020) conducted a review on the application of SA in BPA, summarizing key insights into its implementation in this field. Shen and Yarnold (2021) conducted a scaled Morris-based SA to evaluate the energy-structural performance of buildings, integrating Python with EnergyPlus and Abaqus. In a similar study, Maučec et al. (2021) utilized Morris-based SA to assess the performance of a prefabricated timber building, employing SimLab and jEPlus. Additionally, Yang et al. (2021) utilized TRNSYS for LSA, examining the connection between building energy use and thermal comfort. Similarly, Huo et al. (2021) conducted regression-based SA to assess cooling demand and shading performance in nearly zero-energy buildings in China using SimLab. Additionally, Goffart and Woloszyn (2021) compared Random Balance Design Fourier Amplitude Sensitivity Test (RBD-FAST) with Morris screening using the Python Sensitivity Analysis Library (SALib) for building performance simulations. Their study found that EASI RBD-FAST offers greater effectiveness and ease of implementation compared to Morris screening. Furthermore, Chambers et al. (2021) conducted Saltelli sampling and Sobol SA using SALib for a geospatial model of cost-optimal heat electrification in buildings in Switzerland.

Yip et al. (2021) investigated the impact of courtyards, passive and active design strategies, and building-integrated photovoltaic and thermal (BIPV/T) systems on total building energy consumption in net zero energy buildings using TRNSYS, Python, and the modeFRONTIER multi-disciplinary design optimization platform. In another study, Zeferina et al. (2021) applied Morris and Sobol index techniques to conduct SA on the cooling requirements of an office building using jEplus. Similarly, Delgarm et al. (2018) conducted variance-based GSA on the energy performance of a building utilizing EnergyPlus, jEPlus, and MatLab. Baghoolizadeh et al. (2023a, b) employed jEPlus for SA and jEPlus + EA for multi-objective optimization of architectural specifications and control parameters for a smart shadow curtain. In another study, they utilized EnergyPlus to conduct SA and optimization of a building's total heating and cooling loads and associated costs across different climatic conditions using response surface methodology Baghoolizadeh et al. (2021). Additionally, Baghoolizadeh et al. (2022) conducted multi-objective optimization to decrease annual electricity consumption and increase electricity production using photovoltaic shadings on building windows with EnergyPlus. They employed Morris sensitivity analysis (MSA) to assess the impact of design variables on objective functions and established relationships using regression modeling with GMDH type-ANN. In recent research, Baghoolizadeh et al. (2023a, b) utilized jEPlus for SA using the Morris method and jEPlus + EA for multi-objective optimization via NSGA-II. Their aim was to lower both CO_2 concentration and CO_2 pollutant levels while improving thermal comfort for building occupants. In another study, they employed the Grasshopper to model, analyze, and optimize daylight illuminance and energy usage intensity in Tehran office spaces (Hakimazari et al. 2024).

2 Objectives

The background highlights that while many studies have examined SA in building performance, most emphasize LSA for its simplicity and efficiency. Building designers often use established SA software such as jEPlus, SimLab, SALib, modeFRONTIER, or manually iterate through building simulation software to assess outputs, despite their limitations. The limitations of current SA software encompass various factors, including the selection and quantity of inputs for tackling mixed-integer programming (MIP) problems simultaneously. Additionally, constraints such as the type and quantity of outputs, the choice of SA method based on input–output characteristics, boundary conditions, and constraints are critical shortcomings. Moreover, SA software developed across various programming languages necessitates integration with simulation engines, resulting in prolonged computation times. Consequently, researchers have faced considerable delays in completing SA studies due to these extended processing durations. Furthermore, owing to the complexities and challenges associated with programming, only a small number of studies have focused on the numerical enhancement of SBSA for building systems. The current research introduces an innovative and efficient approach for conducting SBSA on building systems. This method not only enables building engineers to predict and analyze how building performance varies with changes in design parameters but also enhances building productivity by facilitating accurate decision-making during the conceptual design phase. To achieve this goal, a novel approach integrates EnergyPlus directly with LSA and GSA algorithms using the C++ programming language. A residential building in Bushehr, Iran, situated in a hot semi-arid climate, serves as a case study to evaluate the effectiveness of this integrated approach. In the OAT, a novel sensitivity analysis index is introduced to assess the impact of inputs on outputs. The main objectives and contributions of this research are outlined below:

- Development of a novel command-line interface using the C++ programming language to directly integrate with EnergyPlus. This advancement enables precise control and significantly enhances computational speed for conducting parametric analysis, sensitivity analysis, multi-objective optimization, uncertainty analysis, and related tasks.
- Addressing limitations inherent in existing interface software, such as popular tools like jEPlus, by offering greater flexibility in selecting building outputs, input parameters, algorithms, and variables.
- Simultaneous implementation of both LSA and GSA methods.
- Introduction of a novel sensitivity analysis index, enhancing analytical capabilities and providing deeper insights into parameter impacts.
- Method implementation designed to be adaptable across diverse building types and configurations, demonstrating its universal applicability in building performance analysis.

To the authors' knowledge, no similar research has been found that presents a practical method for SBSA by integrating a high-level object-oriented programming language directly with EnergyPlus. This approach enhances EnergyPlus capabilities to conduct SA without requiring additional plugins or third-party tools. Given the pivotal role of SBSA in evaluating efficiency and comfort criteria in buildings, existing literature in this domain appears insufficient and necessitates further exploration.

3 Methodology

3.1 LSA method

Basing on the OAT method, each input parameter is systematically varied across its entire allowable range while holding other inputs constant at their nominal values. This approach entails measuring the corresponding outputs for each variation, thereby generating an output versus input change graph. To quantify the sensitivity of outputs to individual inputs, the authors proposed the Dispersion Index (DI). DI_i is defined as the ratio of the standard deviation of outputs (σ) to the average of outputs ($\overline{Y}$), expressed mathematically as:

$$DI_i = \frac{\sigma}{\overline{Y}} \times 100 \quad (1)$$

A higher DI signifies greater variability in the output, indicating a stronger impact of the input on the output's sensitivity. In simpler terms, it shows that changes in the input parameter have a more significant effect on the output.

3.2 GSA method

Rather than analyzing how individual inputs affect system behavior one at a time, GSA simultaneously assesses the impact of changing all inputs together, taking into account their interactions, and quantifying their respective contributions to the variability observed in the system's output. In this study, Sobol's analysis is utilized to categorize the inputs based on their significance and impact on the outputs. Consider a function $Y = f(X)$ that defines the system's behavior based on inputs ($X = [x_1, x_2, \ldots, x_m]$). Sobol's analysis algorithm proceeds in three main steps as follows (Saltelli et al. 2007):

Step 1

Decompose the total variance of the function $Y = f(X)$, which involves m inputs, into conditional variances.

$$V(Y) = \sum_{i}^{m} D_i + \sum_{i}^{m} \sum_{j>i}^{m} D_{ij} + \ldots + D_{1,2,3,\ldots,m} \tag{2}$$

The equation presented above describes V(Y) as the total variance of the function Y. Here, D_i represents the first-order impact of each x_i, while D_{ij} to $D_{1,2,3,\ldots,\mathrm{m}}$ indicate the effects of input interactions, computed as follows:

$$D_i = V[E_{X_{-i}}(Y|X_i)] \tag{3}$$

$$D_{ij} = V\left[E_{X_{-i}}\left(Y|X_i, X_j\right)\right] - V_i - V_j \tag{4}$$

$$D_{ijk} = V\left[E_{X_{-i}}\left(Y|X_i, X_j, X_k\right)\right] - V_i - V_j - V_k \tag{5}$$

and so on. Additionally, E and V denote the expected value and variance, respectively. $E(Y|X_i)$ represents the conditional expectation, with $V[E(Y|X_i)]$ termed as the primary impact of X_i on Y. $E[V(Y|X_{-i})]$ denotes the residual, where X_{-i} refers to all inputs except X_i. Furthermore, $V[E_{X_{-i}}(Y|X_i)]$ signifies the anticipated reduction in output variance, while $E_{X_{-i}}[V(Y|X_{-i})]$ represents the residual output variance expected when X_i is fixed at its nominal value.

Step 2

To compute (Y), $V[E_{X_{-i}}(Y|X_i)]$ and $E_{X_{-i}}[V(Y|X_{-i})]$ using quasi-Monte Carlo estimators, two independent matrices A and B are generated using Sobol quasi-random sequences. Each matrix has M rows and m columns, where M represents the sample size of the sequences, and m denotes the number of input variables. Matrix C_i is created by integrating matrices A and B in a way that retains all columns from A, while replacing the i^{th} column of A with the i^{th} column of B. Consequently, the system produces outputs ${Y_A}^{(m)}$, ${Y_B}^{(m)}$, and ${Y_C}^{(m)}$ based on the inputs derived from matrices A, B, and C. This process facilitates the determination of $V(Y)$, $V[E_{X_{-i}}(Y|X_i)]$, and $E_{X_{-i}}[V(Y|X_{-i})]$ as outlined (Saltelli et al. 2010):

$$V(Y) = \frac{1}{M}\sum_{j=1}^{M}\left[Y_A^{(m)}\right]^2 - \left[\frac{1}{M}\sum_{j=1}^{N} Y_A^{(m)}\right]^2 \tag{6}$$

$$V[E_{X_{-i}}(Y|X_i)] = V(Y) - \frac{1}{2M}\sum_{j=1}^{M}\left[Y_B^{(m)} - Y_{C_i}^{(m)}\right]^2 \tag{7}$$

$$E_{X_{-i}}[V(Y|X_{-i})] = \frac{1}{2M}\sum_{m=1}^{M}\left[Y_A^{(m)} - Y_{C_i}^{(m)}\right]^2 \tag{8}$$

In this work, M of 2000 and m of 12 columns are used to evaluate aforementioned relations.

Step 3

Compute the total-order SI (S_{Ti}):

$$S_{Ti} = \frac{E_{X_{-i}}[V(Y|X_{-i})]}{V(Y)} \tag{9}$$

The greater the S_{Ti}, the more influential the input is on the system output. The S_{Ti} quantifies the cumulative effect of an input on the system outputs, accounting for all interactions with other inputs, and reveals the proportion of variance that would persist if uncertainty in all inputs except X_i were eliminated.

3.3 Integrating workflow

Figure 1 indicates the integrating workflow for SBSA of building efficiency, integrating LSA and GSA with EnergyPlus, released by the U.S. Department of Energy's (DOE) Building Technologies Office (BTO) (EnergyPlus 2024), for iterative simulations. As indicated in Fig. 1, the inputs for the proposed model consist of weather data, building design parameters, output variables, input variables whose influences on the output variables are to be studied, and the range of input variables (constraints). EnergyPlus relies solely on input/output data. Accordingly, to address the SBSA challenge, a novel approach was introduced: command-line functions were developed using the C++ programming language. These functions are designed to initiate EnergyPlus and execute simulations based on randomly generated inputs $[(X_i)]$ derived from Sobol quasi-random sequences, alongside weather data and a building model. Subsequently, the simulation outputs $([F(X_i)])$ from EnergyPlus are gathered for further post-processing. The OAT and Sobol's analyses algorithms have been implemented using the C++ programming language to assess the achieved $[F(X_i)]$. The OAT analysis provides insights into the output trends in response to changes in individual inputs and calculates the DI for each output with respect to each input, without considering interactions with other inputs. On the other hand, Sobol's analysis calculates the total-order SI (S_{Ti}) for each output with respect to each input, taking into account the interactions of input changes simultaneously. Therefore, this paper introduces an innovative approach where SA is integrated directly into EnergyPlus, eliminating the need for external plugins or third-party tools. This integration significantly enhances computational speed and efficiency. It is worth noting that in Fig. 1, the red arrow is used for the optimization process (and not for the implementation of the sensitivity analysis process), which will be the focus of authors' future research. While extensive research has delved into the SA of building performance, there remains

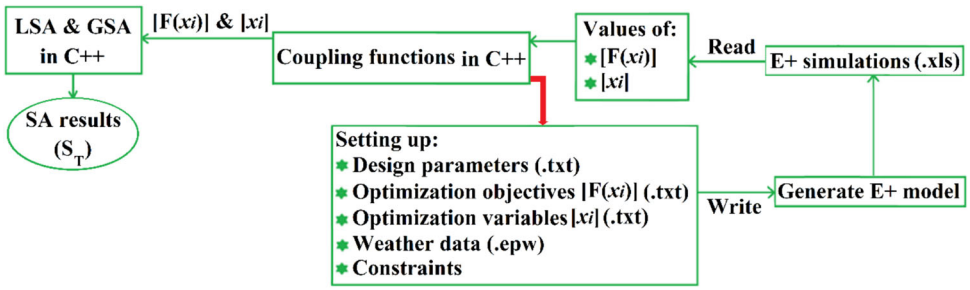

Fig. 1 Integrating workflow

a conspicuous lack of studies that outline a practical and structured approach for SBSA through direct coupling of a high-level programming language with building simulation software.

In this context, a novel initiative integrates LSA and GSA directly with EnergyPlus using C++ , a powerful object-oriented programming language. This integration enhances EnergyPlus with the capabilities of C++ , enabling the application of various SA algorithms, flexible inputs and outputs, and diverse constraints within the framework.

4 Case study

4.1 Building characteristics

The newly devised SBSA methodology is applied to a residential dwelling situated in Iran's hot semi-arid climate to explore its capabilities and potential. Figure 2 illustrates the schematic representation of the building model, which was designed using SketchUp 3D design software (SketchUp 2024). This dwelling accommodates five occupants and measures 3 m in height, with dimensions of 10 m in both length and width. The building's primary facade (BF) faces northward, and it rotates counterclockwise in orientation. The northern, eastern, western, and roof facets of the building are exposed to direct sunlight (SunExposed and WindExposed), while the floor and southern facet are assumed to be adiabatic. No shading elements are present affecting the building. The building includes an east-facing fixed double-glazed window, measuring 1.5 m wide and 4 m long (with a WWR of 20%). The window features 3 mm clear glazing and an argon 6 mm gas gap. Additionally, there is a wooden door on the eastern side, measuring 1.5 m tall and 2 m wide. A flat shading device, 4 m long and 1 m deep, is positioned above the window without any curtains. The shading surface extends directly above the window with no height, left, or right extensions, and is tilted at 90° from the window plane. Table 1 details the material

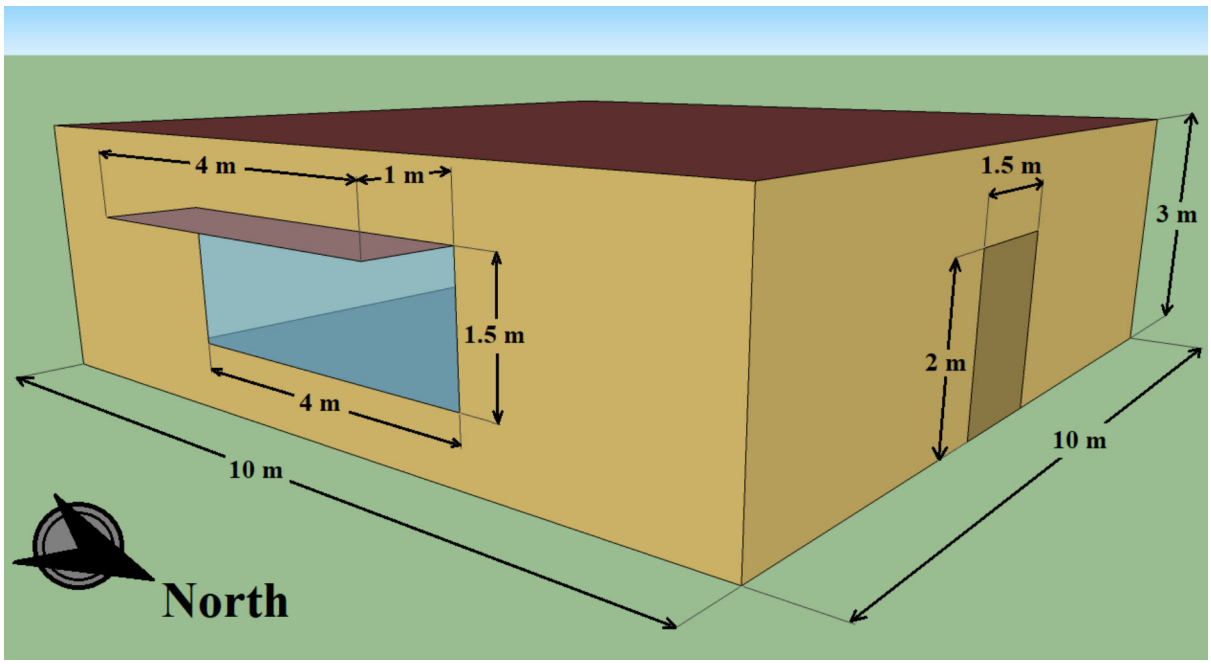

Fig. 2 Schematic representation of the building model

Table 1 Characteristics of the investigated building envelope

Envelope	Specification		Value
Wall	Exterior layer (brick)	Conductivity (W/mK)	0.89
		Thickness (m)	0.1016
		Specific heat (J/kgK)	790
		Density (kg/m^3)	1920
	Interior layer (Wood shingles)	Conductivity (W/mK)	0.04
		Thickness (m)	0.0064
		Specific heat (J/kgK)	1300
		Density (kg/m^3)	592
Floor	Exterior layer (heavyweight concrete)	Conductivity (W/mK)	1.95
		Thickness (m)	0.3048
		Specific heat (J/kgK)	900
		Density (kg/m^3)	2240
	Interior layer (Terrazzo)	Conductivity (W/mK)	1.8
		Thickness (m)	0.0254
		Specific heat (J/kgK)	790
		Density (kg/m^3)	2560
Roof	Exterior layer (lightweight concrete block)	Conductivity (W/mK)	0.49
		Thickness (m)	0.1524
		Specific heat (J/kgK)	800
		Density (kg/m^3)	512
	Middle layer (gypsum)	Conductivity (W/mK)	0.16
		Thickness (m)	0.0159
		Specific heat (J/kgK)	1090
		Density (kg/m^3)	800
	Interior layer (Wood shingles)	Conductivity (W/mK)	0.04
		Thickness (m)	0.0064
		Specific heat (J/kgK)	1300
		Density (kg/m^3)	592
Door	Exterior layer (Wood)	Conductivity (W/mK)	0.15
		Thickness (m)	0.0127
		Specific heat (J/kgK)	1630
		Density (kg/m^3)	608
Window	Double 2.5 mm clear glazing	Solar transmittance	0.85
		Visible transmittance	0.901
		Conductivity (W/mK)	0.9
		Thickness (m)	0.0025

specifications utilized in constructing the investigated building. Additionally, a Variable Air Volume (VAV) system predefined in the EnergyPlus has been integrated into the building, designed to deliver an outdoor airflow rate of 9.5 l/s per person. This system dynamically adjusts its capacity in response to the varying climatic conditions experienced throughout the year. In accordance with guidelines from the United States Environmental Protection Agency (EPA 2009), the optimal cooling and heating setpoint temperatures have been determined to achieve a balance between energy conservation and occupant comfort. Specifically, the recommended setpoints are approximately 24.5 °C for cooling and 21 °C for heating, ensuring thermal comfort for a significant majority of building occupants.

To regulate indoor lighting conditions, an illuminance threshold of 500 lx has been set, adhering to the EN 12464-1 standard for office environments (European Committee for Standardization 2011). Moreover, various operational schedules such as clothing, lighting usage, occupancy patterns, air velocity, and infiltration rates have been meticulously defined based on the specifications provided by the EnergyPlus dataset (EnergyPlus 2024). These parameters are crucial for accurately simulating and

evaluating the building's energy performance and indoor environmental quality under different scenarios and conditions.

4.2 Weather condition

Iran is located in Western Asia, covering approximately 1.65 million km^2 along the coastlines of the Sea of Oman and the Persian Gulf to the south. Iran experiences a hot-dry climate characterized by extended hot and dry summers and brief cool winters. Bushehr, a port city on the southern coast of Iran along the Persian Gulf, has a hot semi-arid climate. Temperatures in Bushehr range from 12 °C to 37 °C annually, with rare occurrences falling below 9 °C or exceeding 40 °C (Iran Meteorological Administration 2019–2023). The city is positioned at a latitude of 28.9036N and a longitude of 50.8208E. Bushehr experiences 217 annual heating degree-days (HDDs) and 2847 annual cooling degree-days (CDDs) based on an 18.3°C threshold (ASHRAE 2009/2013/2017/2021). For this study, Bushehr serves as the representative city for the selected climate region, and weather data in EPW format provided by DOE BTO is utilized for EnergyPlus simulations.

4.3 Inputs, outputs, and constraints

This study incorporates four output variables: AHC, ACC, ALC, and PPD, which assesses occupant thermal comfort levels. Additionally, the following inputs are considered: building rotation from the north axis (BR), window-to-wall ratio (WWR), depth of shading device (DSH), cooling and heating setpoints (CSPT and HSPT), solar absorptance of interior walls (SA_{IN_W}) and exterior walls (SA_{Ex_W}), thickness of exterior walls (Th_{Ex_W}), solar transmittance of window glass (ST_{win}), visible transmittance of window glass (VT_{win}), thickness of window glass (ST_{win}), and thickness of gas in the window ($Th_{gas-win}$). The selected parameters cover a broad spectrum that directly impacts key aspects of building performance, including AHC, ACC, ALC, and PPD. Factors such as building orientation, window-to-wall ratio, shading depth, and cooling/heating setpoints exert significant influence on building energy demand, affecting heating and cooling loads, and consequently influencing overall energy consumption and operational costs. Window properties, such as solar absorption of building walls (internal and external), solar transmittance coefficient of window glass, and visible transmittance of window glass, impact daylight penetration and artificial lighting requirements. Optimization of these parameters enhances lighting efficiency, thereby reducing energy use for illumination. Moreover, building wall thickness, coefficient of thermal resistance of window glass, and the thickness of gas layers in windows are crucial for maintaining thermal comfort, affecting indoor temperature fluctuations, HVAC operation requirements, and occupant comfort and productivity. Our methodology ensures systematic variation of these parameters within defined ranges to comprehensively assess their individual and collective effects on building performance, thereby enhancing the robustness and reliability of our developed method and sensitivity analysis findings. Therefore, these parameters were selected to evaluate their influence on the functional behavior of the building through the proposed method. The specifications of the inputs are given in Table 2.

5 Verification

To validate the developed method, a widely used software among researchers was selected. jEPlus, provided by Dr. Yi Zhang (jEPlus 2024), is a parametric study tool for buildings that runs both EnergyPlus and TRNSYS software. By discretely running EnergyPlus, jEPlus allows for the examination of the building model under various desired design parameters. The inputs for jEPlus consist of the building model simulated in EnergyPlus (.idf format), a Bushehr city weather file (.epw format), discretely defined input variables (.csv format), and output variables (.txt format). The outputs generated by jEPlus are stored in an Excel file format. For this study, the inputs included the building rotation as an input with 16 discrete values and the AHC as the output variable. These inputs and outputs were prepared were prepared and fed into jEPlus. Figure 3 illustrates a comparative analysis between the outcomes generated by the proposed method and those produced by jEPlus. As demonstrated, the values obtained from jEPlus

Table 2 Characteristics of the inputs

Input	Unit	Initial value	Range
B R	°	0	[0,360)
WWR	–	0.2	(0,1)
DSH	m	1	(0,1.5]
CSPT	°C	24.5	(22,33]
HSPT	°C	21	[13,22]
SA_{IN_W}	–	0.505	[0,1]
SA_{Ex_W}	–	0.311	[0,1]
Th_{Ex_W}	m	0.1	[0.1,0.4]
ST_{win}	–	0.837	[0,1]
VT_{win}	–	0.898	[0,1]
Th_{win}	mm	3	[1,16]
$Th_{gas-win}$	mm	6	[1,14]

align precisely with the results from the proposed method, indicating no discrepancies. This consistency arises because both the developed method and jEPlus leverage the EnergyPlus engine, thereby producing identical outcomes. Nevertheless, the primary distinction lies in the fact that the developed programming methods enable researchers to conduct a diverse array of analyses on the building model. In contrast, existing commercial software imposes substantial limitations on the scope of analyses that can be performed. This flexibility is particularly advantageous in large-scale optimization projects or scenarios requiring extensive iterative simulations to explore various design alternatives.

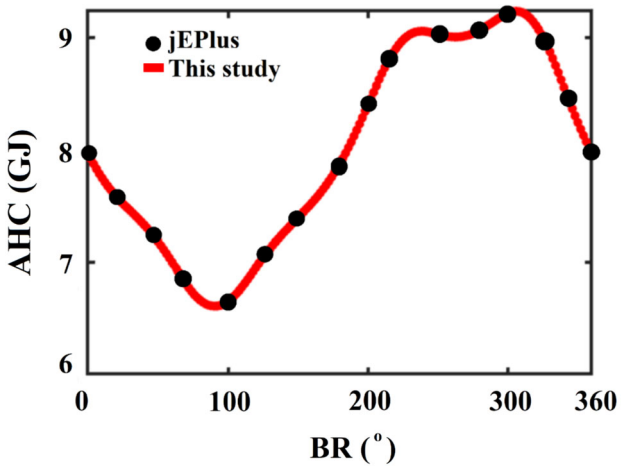

Fig. 3 Comparative analysis between the developed method and jEPlus

Additionally, the comparative analysis highlighted a significant reduction in computational time when employing the developed method as compared to jEPlus. The proposed method calculated the AHC for 500 different building rotation angles, ranging from 0 to 360 degrees, in just 36 s and automatically generated the corresponding plot. In contrast, jEPlus, excluding the time required for setup and the post-processing of outputs in Excel for plotting, took approximately 104 s to compute the AHC for the same 500 rotation angles and 11 s only for 16 building rotation angles. This reduction in computational time not

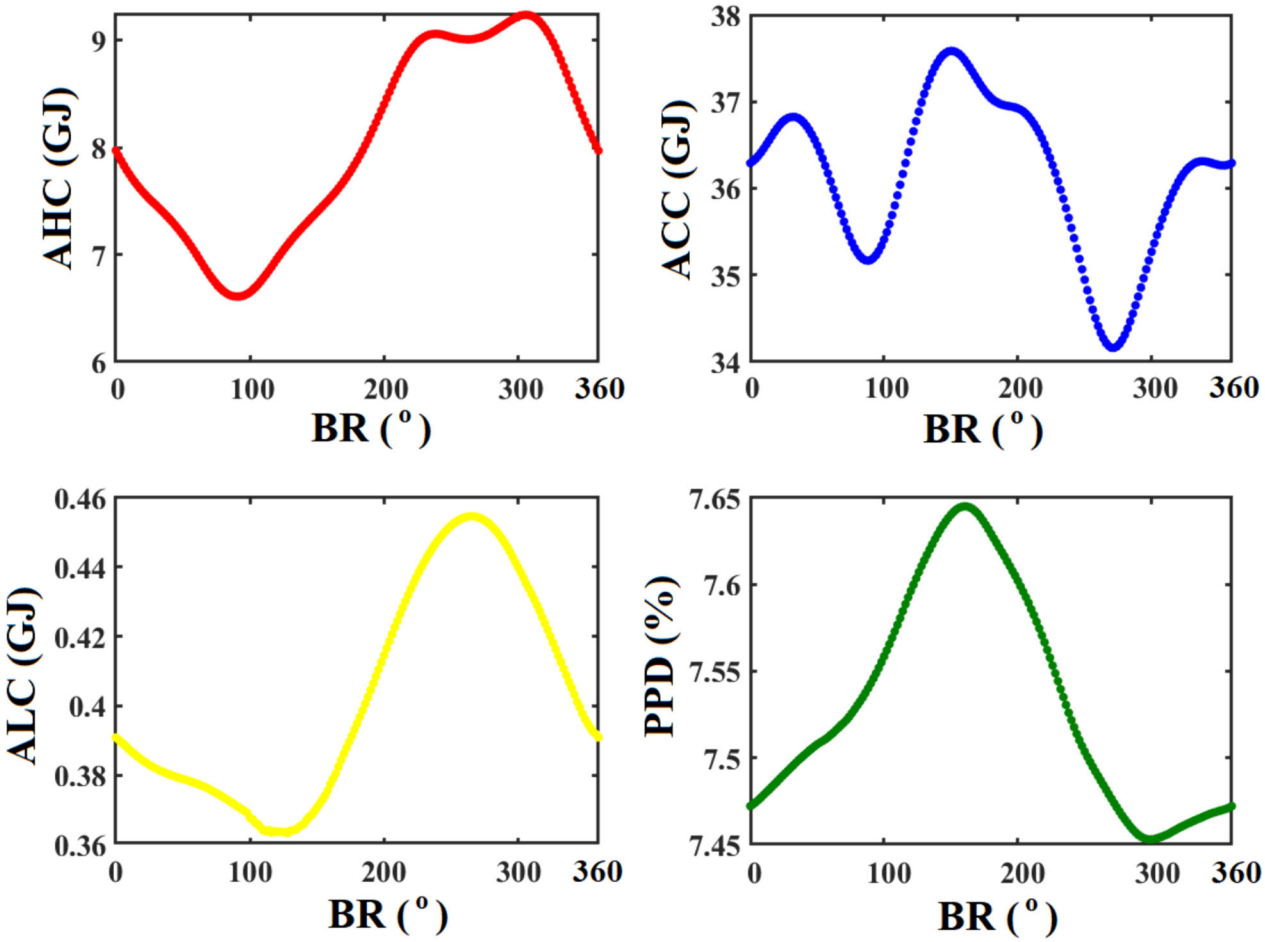

Fig. 4 Impact of BR on the AHC, ACC, ALC, and PPD

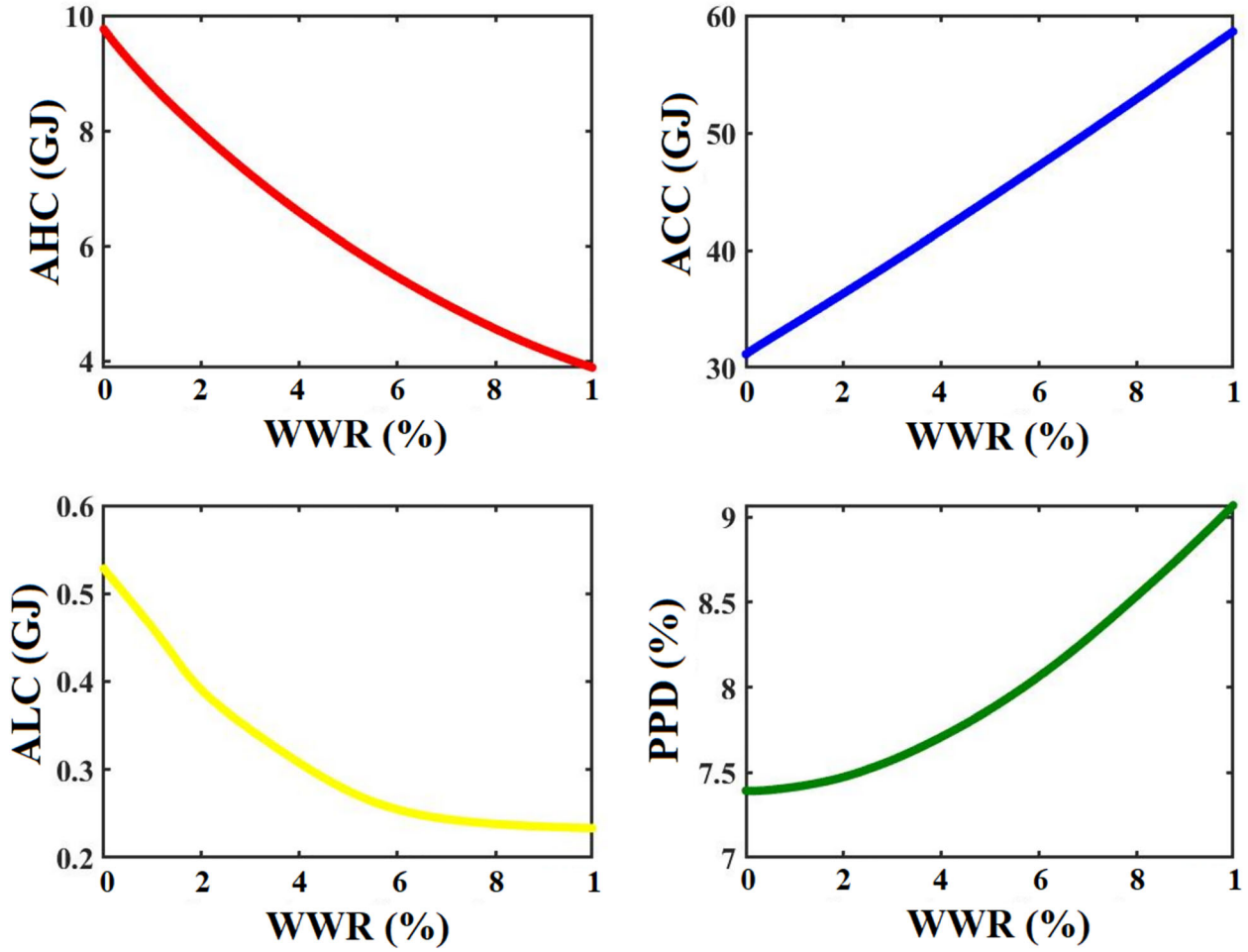

Fig. 5 Impact of WWR on the AHC, ACC, ALC, and PPD

only enhances the feasibility of the developed method for practical applications but also underscores its potential in facilitating more efficient building simulations. This is particularly advantageous in large-scale optimization projects or in scenarios that demand extensive iterative simulations to explore various design alternatives. Overall, the proposed method not only aligns well with established simulation tools in terms of accuracy but also excels in computational efficiency, offering substantial benefits for researchers and practitioners engaged in complex building performance sensitivity analysis and optimization tasks.

6 Results and discussion

In this section, the outcomes of applying the developed method are presented. Initially, OAT analysis, serving as LSA, explores how outputs respond to input variations, along with evaluating the sensitivity of each output to individual inputs, irrespective of other input interactions. Subsequently, Sobol's analysis, as GSA, is conducted to quantify and prioritize the overall sensitivity of outputs to inputs.

6.1 Results of OAT analysis

This phase of the study investigates how BR, WWR, DSH, CSPT, HSPT, SA_{IN_W}, SA_{Ex_W}, Th_{Ex_W}, ST_{win}, VT_{win}, Th_{win}, $Th_{gas-win}$ on the AHC, ACC, ALC, and PPD influence AHC, ACC, ALC, and PPD using the OAT method. Each input variable is individually varied across its entire range while keeping other inputs fixed at their nominal values (as specified in Table 1 and 2), and the corresponding outputs are observed.

6.1.1 Impact of BR

Figure 4 illustrates the impact of BR on the AHC, ACC, ALC, and PPD. The results showed that the lowest values of AHC, ACC, ALC, and PPD were achieved at BR angles of 90° (east-facing), 272° (west-facing), 128° (southwest-facing), and 298° (northeast-facing), respectively. This

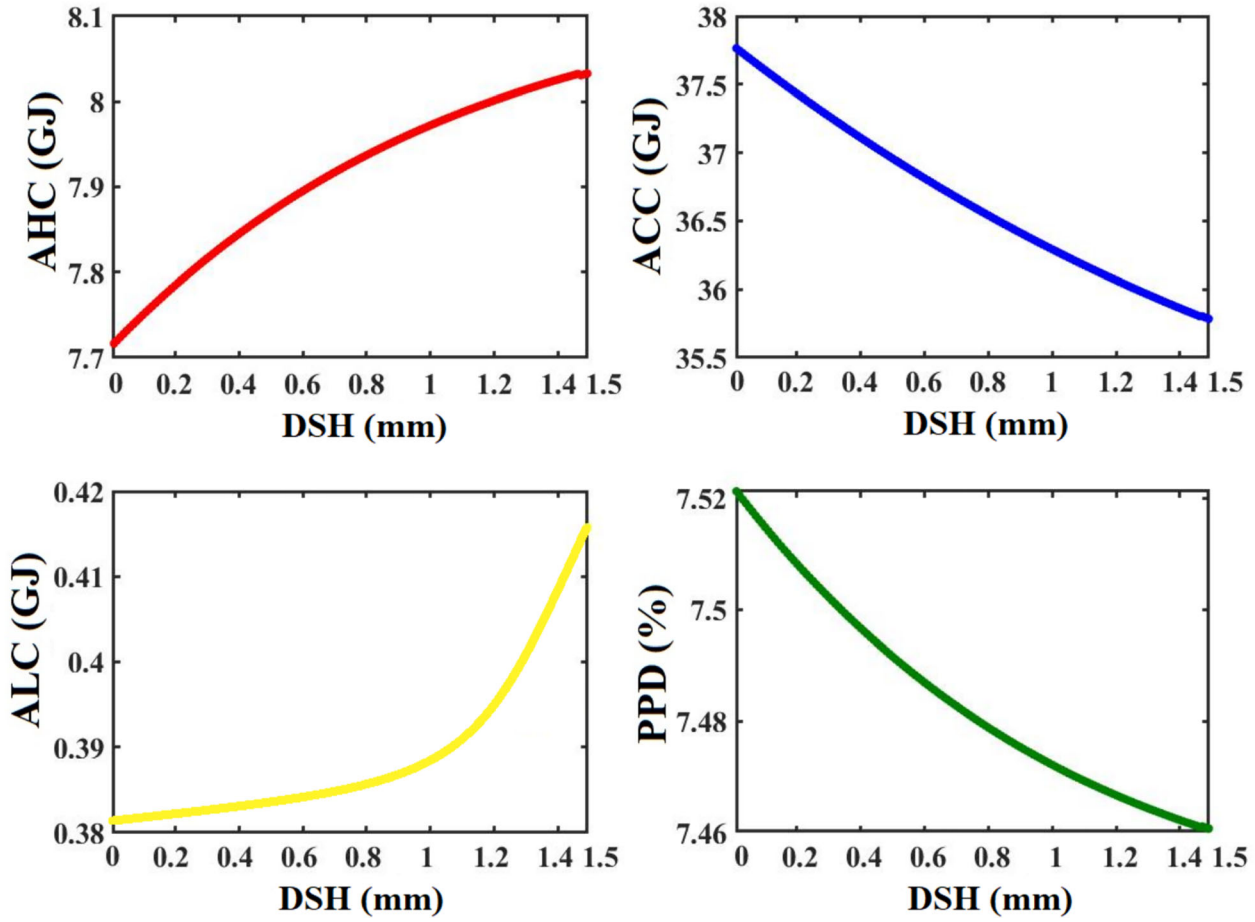

Fig. 6 Impact of DSH on the AHC, ACC, ALC, and PPD

indicates a complex and nonlinear relationship between BR and building performance metrics. Optimal BR values need to be identified through Pareto optimization to simultaneously optimize annual total energy consumption (ATC) and PPD criteria. The sensitivity analysis revealed DI values of 12% for AHC, 3% for ACC, 8% for ALC, and 1% for PPD, highlighting that BR has the greatest influence on AHC and the least influence on PPD, independent of other inputs.

6.1.2 Impact of WWR

Figure 5 indicates the impact of WWR on the AHC, ACC, ALC, and PPD. Increasing WWR results in decreased AHC and ALC, while ACC and PPD increase due to enhanced intake of lighting and heating energy from the external environment into the building. Optimizing WWR requires Pareto analysis to achieve optimal values for both ATC and PPD criteria. The changes in AHC and ACC exhibit a linear relationship with increasing WWR, whereas PPD and ALC changes demonstrate an exponential response to WWR variations. The sensitivity analysis reveals DI values of 27% for AHC, 18% for ACC, 28% for ALC, and 7% for PPD, highlighting that WWR significantly influences AHC and ALC, while its impact on PPD is comparatively minor.

6.1.3 Impact of DSH

Figure 6 indicates the impact of DSH on the AHC, ACC, ALC, and PPD. Increasing DSH leads to higher AHC and ALC, while PPD and ACC decrease due to reduced intake of lighting and heating energy from the external environment into the building. Optimizing DSH requires Pareto optimization to achieve optimal values for both ATC and PPD criteria. Changes in AHC, ACC, ALC, and PPD show an exponential response to variations in DSH. The sensitivity analysis reveals DI values of 2% for AHC, 2% for ACC, 2% for ALC, and 1% for PPD, indicating that DSH has a minimal influence on these variables.

6.1.4 Impact of CSPT

Figure 7 indicates the impact of CSPT on the AHC, ACC, ALC, and PPD. Increasing CSPT results in decreased AHC and ACC, while ALC remains unaffected, indicating its independence from CSPT. Notably, PPD initially decreases

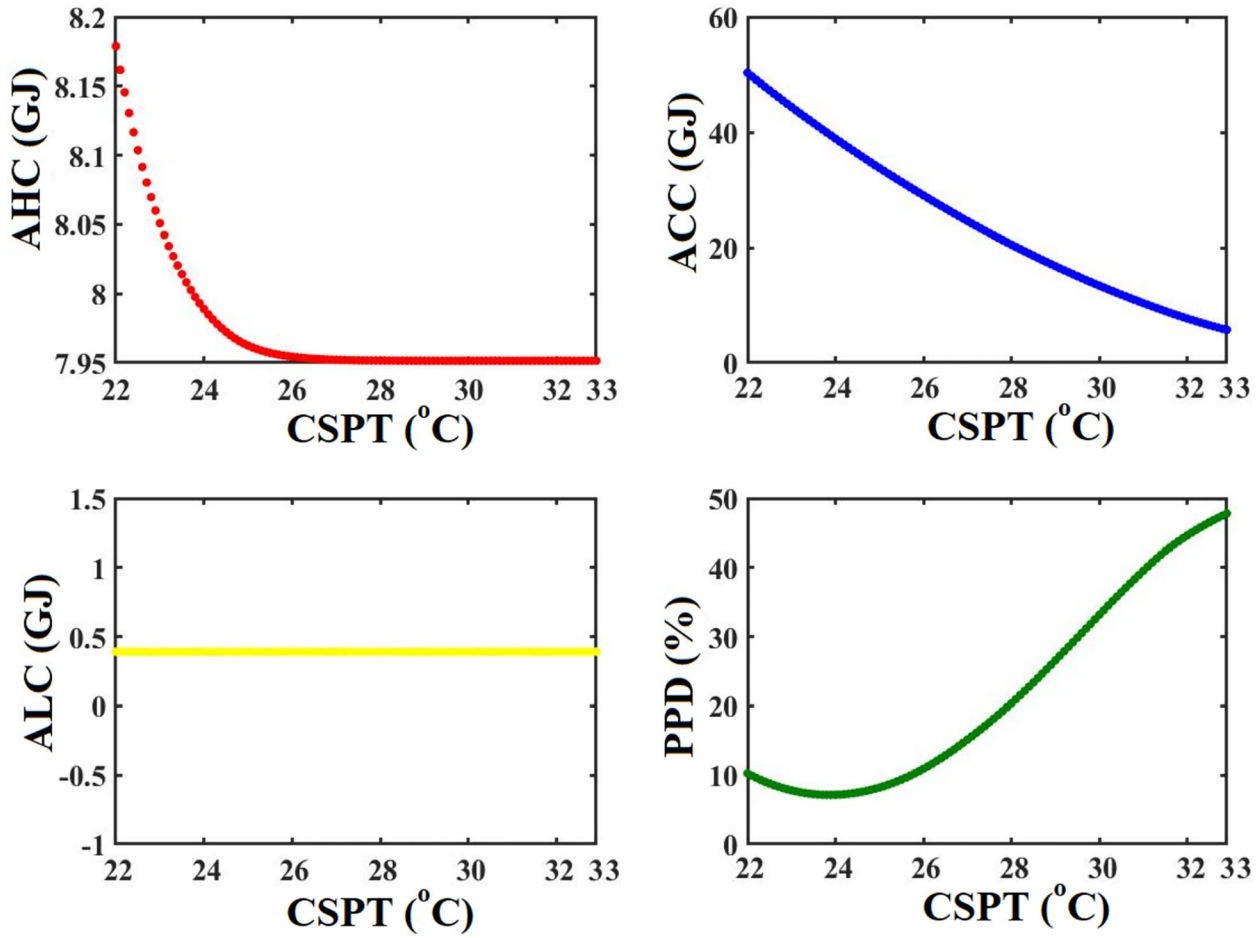

Fig. 7 Impact of CSPT on the AHC, ACC, ALC, and PPD

with increasing CSPT but sharply increases above 24 °C. This trend aligns with the Fanger model (Fanger 1970), where higher CSPT values initially improve thermal comfort conditions, but excessive temperatures above 24 °C delay the VAV system's operation, leading to discomfort among occupants. Despite the reduction in ATC due to delayed VAV system activation at higher CSPT, thermal comfort conditions deteriorate, causing PPD to deviate from optimal levels. The observed trend of PPD versus CSPT also aligns with the recommendations by the (EPA 2009) for optimal thermal comfort. Pareto optimization is essential to identify the optimal CSPT that balances both ATC and PPD criteria effectively. Changes in ACC show a nearly linear response to CSPT variations, while AHC and PPD exhibit exponential and parabolic relationships with CSPT changes, respectively. The sensitivity analysis reveals DI values of 1% for AHC, 54% for ACC, 0% for ALC, and 64% for PPD, highlighting CSPT's significant influence on PPD and ACC, with minimal impact on AHC and ALC.

6.1.5 Impact of HSPT

Figure 8 indicates the impact of HSPT on the AHC, ACC, ALC, and PPD. Increasing HSPT results in increased AHC and ACC, contrasting with the impact of CSPT on these variables. Similar to CSPT, HSPT does not affect ALC, indicating its independence from heating setpoint changes. Furthermore, as HSPT transitions from very cold to moderate temperatures, PPD decreases due to improved thermal comfort conditions based on the Fanger model, approaching optimal levels. The trend of PPD versus HSPT aligns with recommendations by the (EPA 2009) for achieving ideal thermal comfort conditions. AHC and ACC exhibit exponential changes with HSPT variations, whereas PPD changes follow a parabolic pattern.

Pareto optimization is crucial to determine the optimal HSPT that balances both ATC and PPD criteria effectively. The sensitivity analysis reveals DI values of 92% for AHC, 1% for ACC, 0% for ALC, and 22% for PPD, highlighting

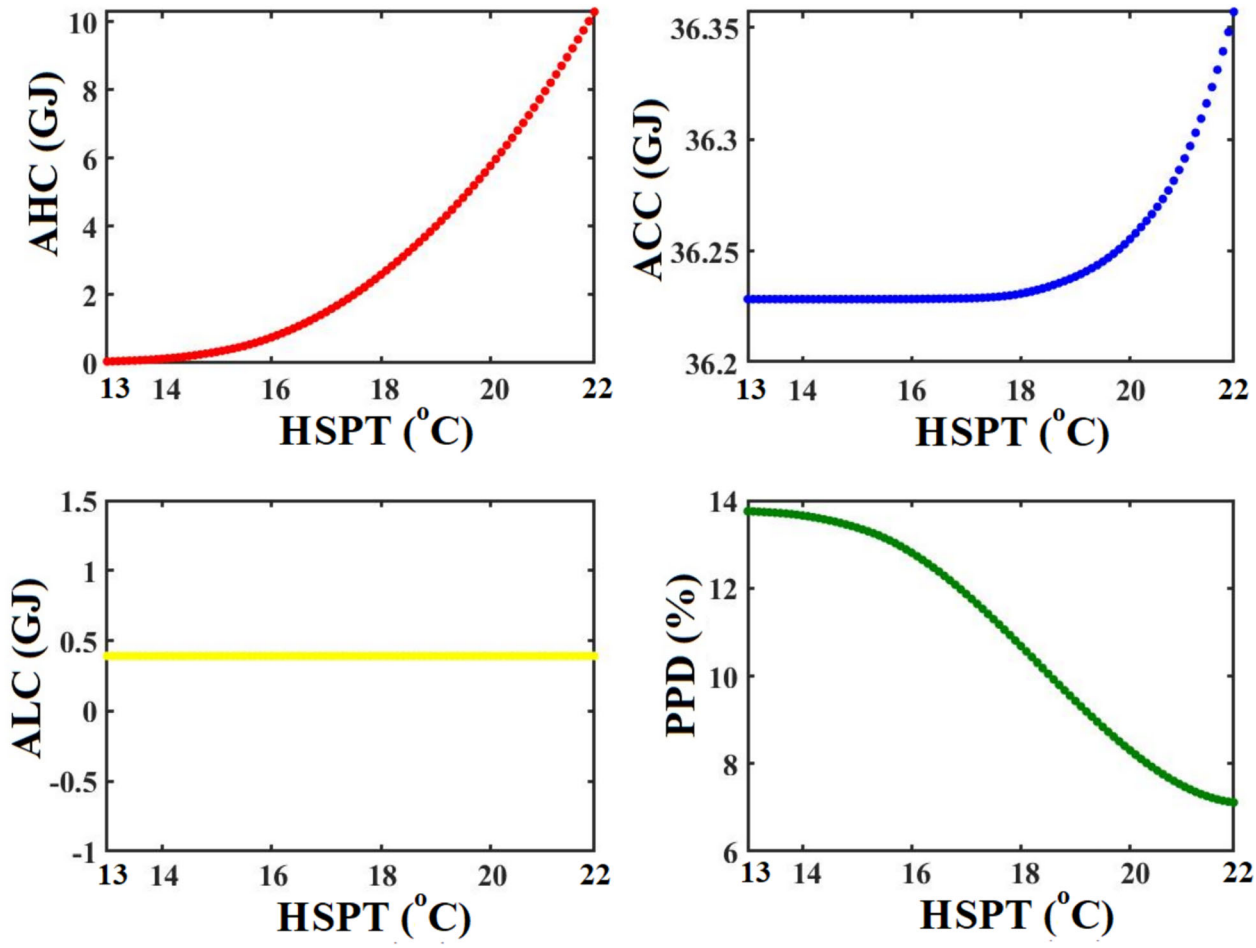

Fig. 8 Impact of HSPT on the AHC, ACC, ALC, and PPD

HSPT's significant influence on AHC and minimal impact on ACC and ALC.

6.1.6 *Impact of* SA_{in_w}

Figure 9 indicates the impact of SA_{in_w} on the AHC, ACC, ALC, and PPD. Increasing SA_{in_w} leads to decreased ACC and PPD, while AHC increases. However, SA_{in_w} has no effect on ALC, indicating its independence from changes in interior wall solar absorptance. Essentially, darker interior wall colors result in reduced ACC and PPD and increased AHC. Pareto optimization is essential to identify the optimal SA_{in_w} that achieves optimal values for both ATC and PPD criteria. Changes in AHC, ACC, and PPD exhibit exponential trends relative to variations in SA_{in_w}. Overall, SA reveals DI values of 1% for AHC, 1% for ACC, 0% for ALC, and 1% for PPD, indicating that SA_{in_w} has minimal influence on these variables.

6.1.7 *Impact of* SA_{ex_w}

Figure 10 indicates the impact of SA_{ex_w} on the AHC, ACC, ALC, and PPD. Increasing SA_{ex_w} results in decreased AHC while ACC and PPD increase. However, SA_{ex_w} shows no effect on ALC, indicating its independence from changes in exterior wall solar absorptance. In essence, darker exterior wall colors lead to lower AHC and higher ACC and PPD. Therefore, a Pareto optimization is necessary to determine the optimal SA_{ex_w} that achieves optimal values for both ATC and PPD criteria. AHC and PPD changes exhibit exponential and parabolic trends, respectively, while ACC changes linearly relative to variations in SA_{ex_w}. Overall, sensitivity analysis reveals DI values of 63% for AHC, 44% for ACC, 0% for ALC, and 20% for PPD, highlighting that SA_{ex_w} primarily influences AHC and has minimal impact on ALC.

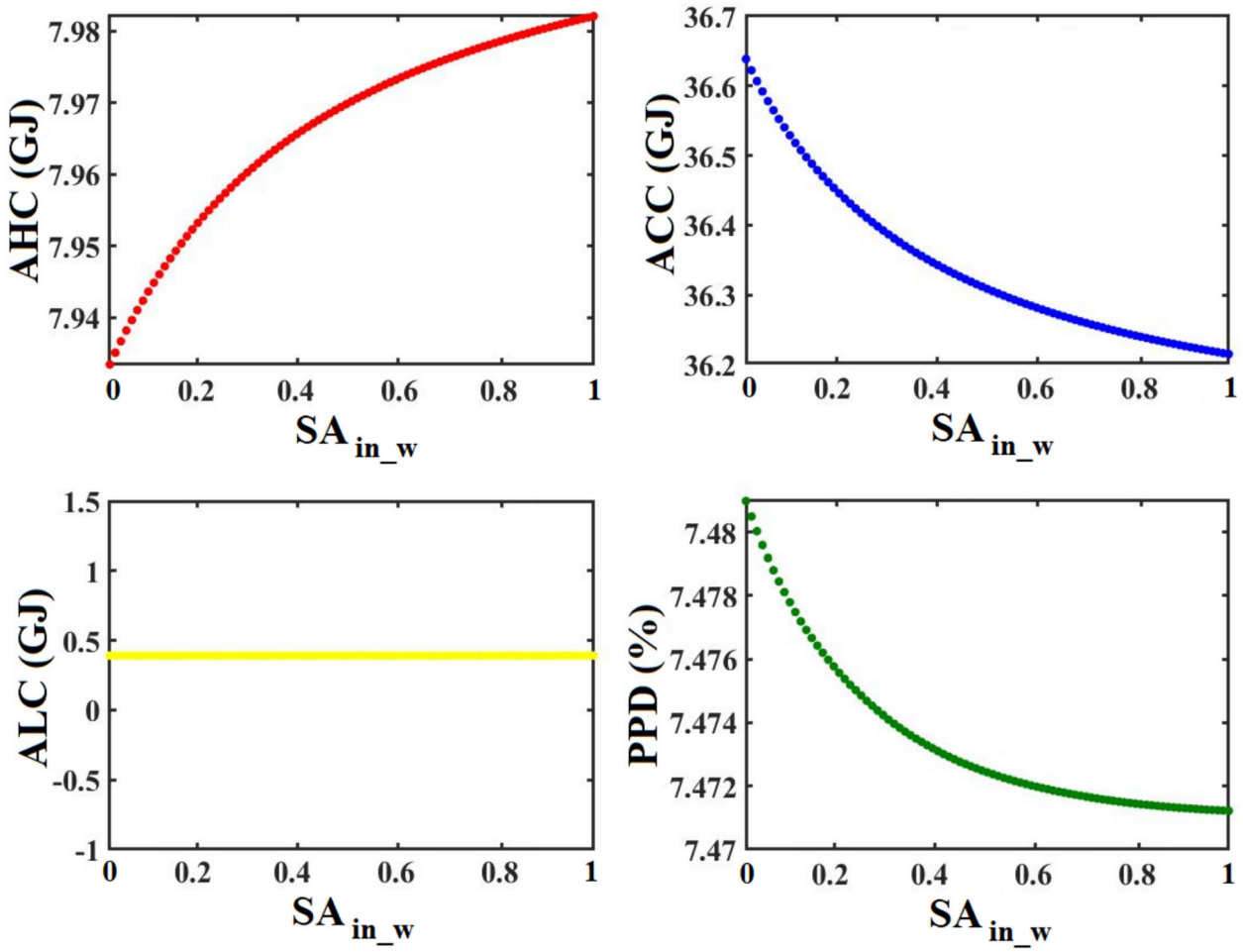

Fig. 9 Impact of $SA_{\text{in\_w}}$ on the AHC, ACC, ALC, and PPD

6.1.8 Impact of $Th_{\text{ex\_W}}$

Figure 11 indicates the impact of Th_{ex_w} on the AHC, ACC, ALC, and PPD. Increasing Th_{ex_w} results in a nearly parabolic decrease in AHC, ACC, and PPD. However, Th_{ex_w} shows no effect on ALC, indicating its independence from changes in wall thickness. Thicker walls provide enhanced insulation, improving energy efficiency, thermal comfort, and soundproofing, which aligns with findings from (Yu et al. 2022). Nevertheless, thicker walls incur additional material costs and weight. Therefore, a comprehensive cost–benefit analysis is essential for determining the optimal Th_{ex_w}. Overall, sensitivity analysis reveals DI values of 10% for AHC, 6% for ACC, 0% for ALC, and 2% for PPD, indicating that Th_{ex_w} primarily influences AHC and has minimal impact on ALC.

6.1.9 Impact of ST_{win}

Figure 12 indicates the impact of ST_{win} on the AHC, ACC, ALC, and PPD. Increasing ST_{win} results in a decrease in AHC, accompanied by an increase in ACC and PPD due to higher solar heat penetration through the window glass. Notably, ALC remains unaffected by changes in ST_{win}. Optimizing ST_{win} to achieve optimal values for both annual total energy consumption (ATC) and PPD requires a Pareto optimization approach. The relationship between ST_{win} and AHC, ACC, and PPD changes is complex, showing a near-parabolic trend. Sensitivity analysis indicates that ST_{win} influences AHC and ACC the most, with DI values of 5% and 4%, respectively. In contrast, its impact on ALC and PPD is minimal, with DI values of 0% and 1%. Despite its relatively modest overall effect, fine-tuning ST_{win} is critical for enhancing building energy efficiency and ensuring occupant comfort.

6.1.10 Impact of VT_{win}

Figure 13 indicates the impact of VT_{win} on the AHC, ACC, ALC, and PPD. Increasing VT_{win} results in a slight increase in AHC, while ACC, ALC, and PPD decrease almost parabolically due to increased lighting energy entering the

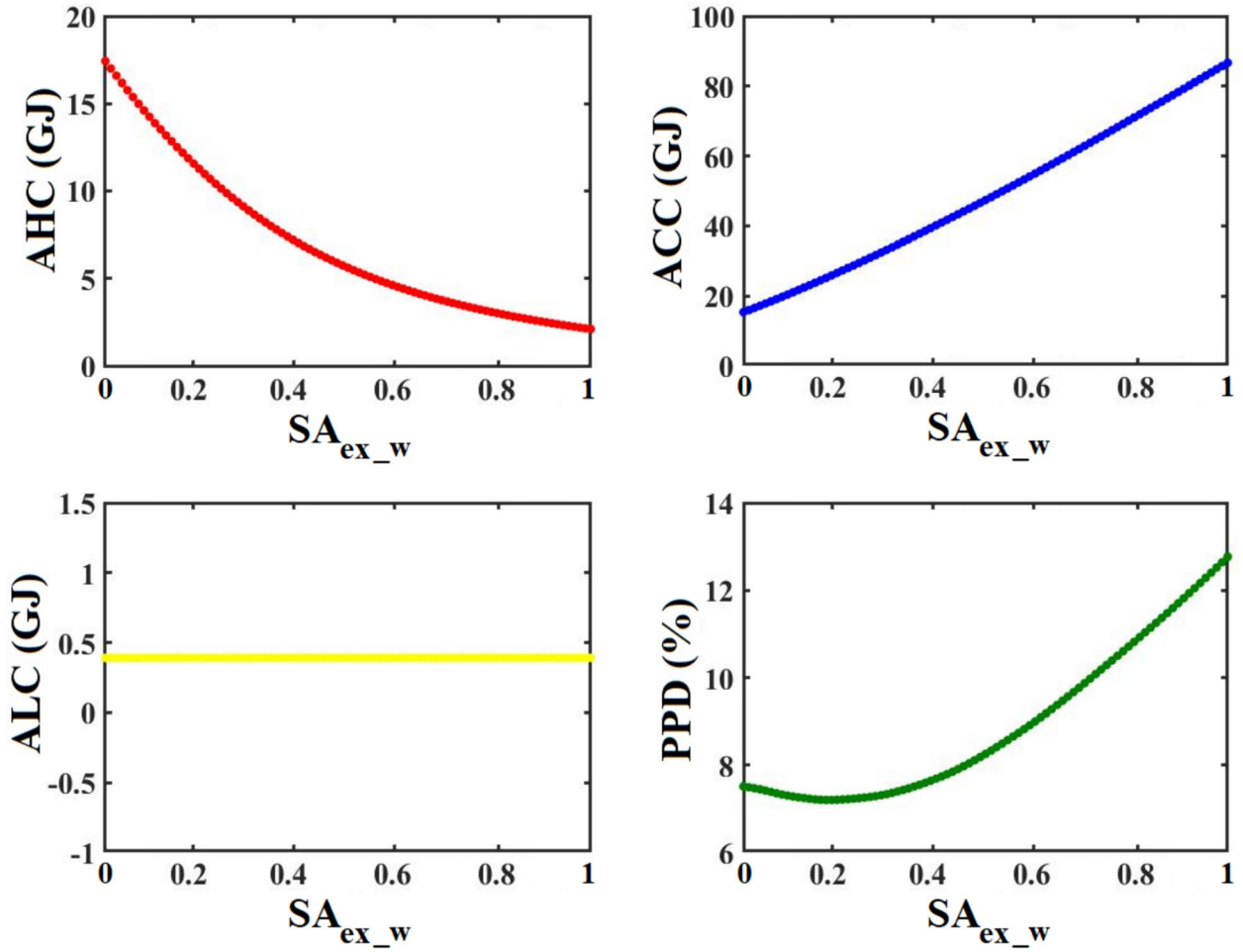

Fig. 10 Impact of SA_{ex_w} on the AHC, ACC, ALC, and PPD

building through the window glass. Optimizing VT_{win} to achieve optimal values for both ATC and PPD necessitates a Pareto optimization approach. The relationship between VT_{win} and AHC, ACC, ALC, and PPD changes is notable for its complex nature, showing a parabolic trend. Sensitivity analysis reveals that VT_{win} has the most influence on ALC, with a DI value of 11%, while its impact on AHC, ACC, and PPD is minimal, with DI values of 1% each.

6.1.11 Impact of Th_{win}

Figure 14 indicates the impact of Th_{win} on the AHC, ACC, ALC, and PPD. The analysis showed that as Th_{win} increases, there is a consistent, albeit slight, linear decrease observed in AHC, ACC, and PPD. This trend suggests that thicker window glass provides enhanced thermal insulation, thereby reducing both heating and cooling energy demands, as well as improving occupant thermal comfort. Interestingly, the study found that Th_{win} does not significantly affect ALC. This implies that the thickness of window glass primarily affects the building's thermal performance rather than its lighting requirements. The observed changes underscore the importance of optimizing Th_{win} to achieve a balance between energy efficiency and indoor environmental quality. The sensitivity analysis conducted through DI values reveals that Th_{win} exerts a relatively small influence on AHC, ACC, ALC, and PPD, with DI values of 1%, 1%, 0%, and 1%, respectively. Despite its modest direct impact, understanding how Th_{win} interacts with other building parameters is crucial for comprehensive building design and energy management strategies. This insight aids in making informed decisions that enhance building performance across various climatic conditions.

6.1.12 Impact of Th_{gas_win}

Figure 15 indicates the impact of $Th_{gas-win}$ on the AHC, ACC, ALC, and PPD. The analysis showed that as $Th_{gas-win}$ increases, there is an exponential decrease observed in annual AHC, ACC, and PPD. This trend

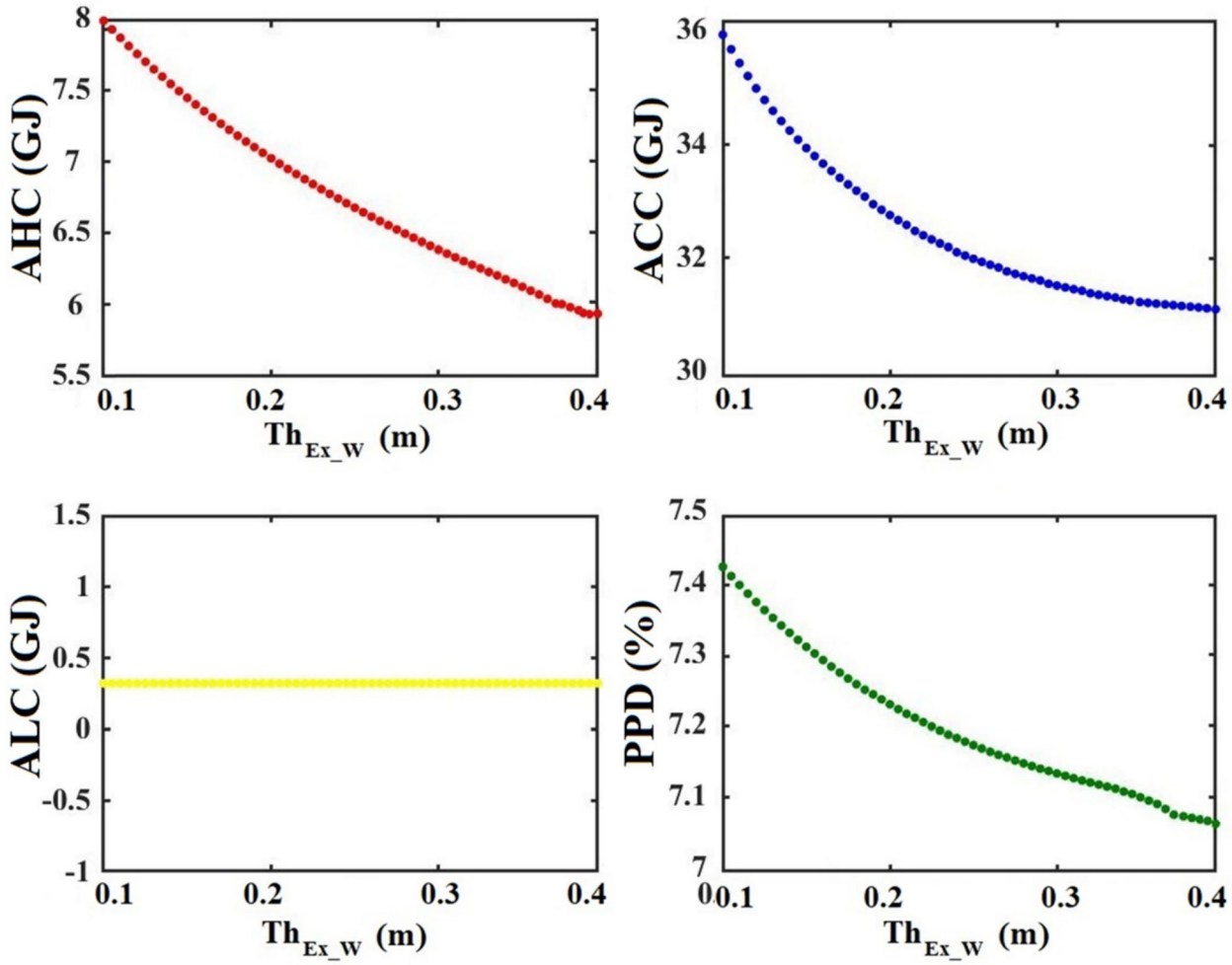

Fig. 11 Impact of Th_{ex_w} on the AHC, ACC, ALC, and PPD

suggests that a thicker gas layer enhances the insulating properties of the window, thereby reducing both heating and cooling energy demands and improving occupant comfort. Interestingly, the study found that $Th_{gas-win}$ does not affect ALC, indicating that changes in the gas layer thickness primarily impact thermal performance rather than lighting requirements. This underscores the importance of optimizing $Th_{gas-win}$ to achieve optimal energy efficiency and indoor environmental quality. The sensitivity analysis conducted through DI values reveals that $Th_{gas-win}$ has a relatively small influence on AHC, ACC, ALC, and PPD, with DI values of 1%, 1%, 0%, and 1%, respectively.

6.2 Results of Sobol's analysis

Table 3 presents S_T basing on Sobol's analysis and DI basing on OAT analysis. It was evident that HSPT, SA_{Ex_W}, and WWR exhibited the highest S_T values, contributing 80%, 79%, and 35% respectively to the variability in AHC. Conversely, DSH, CSPT, SA_{IN_W}, ST_{win}, VT_{win}, Th_{win}, and $Th_{gas-win}$ demonstrated lower influence on AHC. Moreover, B R and Th_{Ex_W} showed moderate influence with S_T values of 16% and 13% respectively on AHC. Additionally, CSPT, SA_{Ex_W}, and WWR showed significant influence on ACC with total-order sensitivity indices S_T of 72%, 63%, and 24% respectively. Conversely, $Th_{gas-win}$,SA_{IN_W},Th_{win}, and VT_{win} demonstrated minimal impact on ACC. Furthermore, WWR, VT_{win}, and B R were identified as the most influential inputs affecting ALC with S_T values of 33%, 25%, and 21% respectively. On the other hand, CSPT, HSPT, SA_{IN_W}, SA_{Ex_W}, Th_{Ex_W}, ST_{win}, Th_{win}, and $Th_{gas-win}$ exhibited no effect on ALC due to the independence of lighting energy use from HVAC system specifications and the thermo-physical properties of walls and window glass. Furthermore, CSPT, HSPT, SA_{Ex_W}, and WWR exhibited significant influence on the PPD, with the S_T of 81%, 40%, 36%, and 28% respectively. Conversely, other parameters considered in the analysis show minimal impact on PPD. Based on the

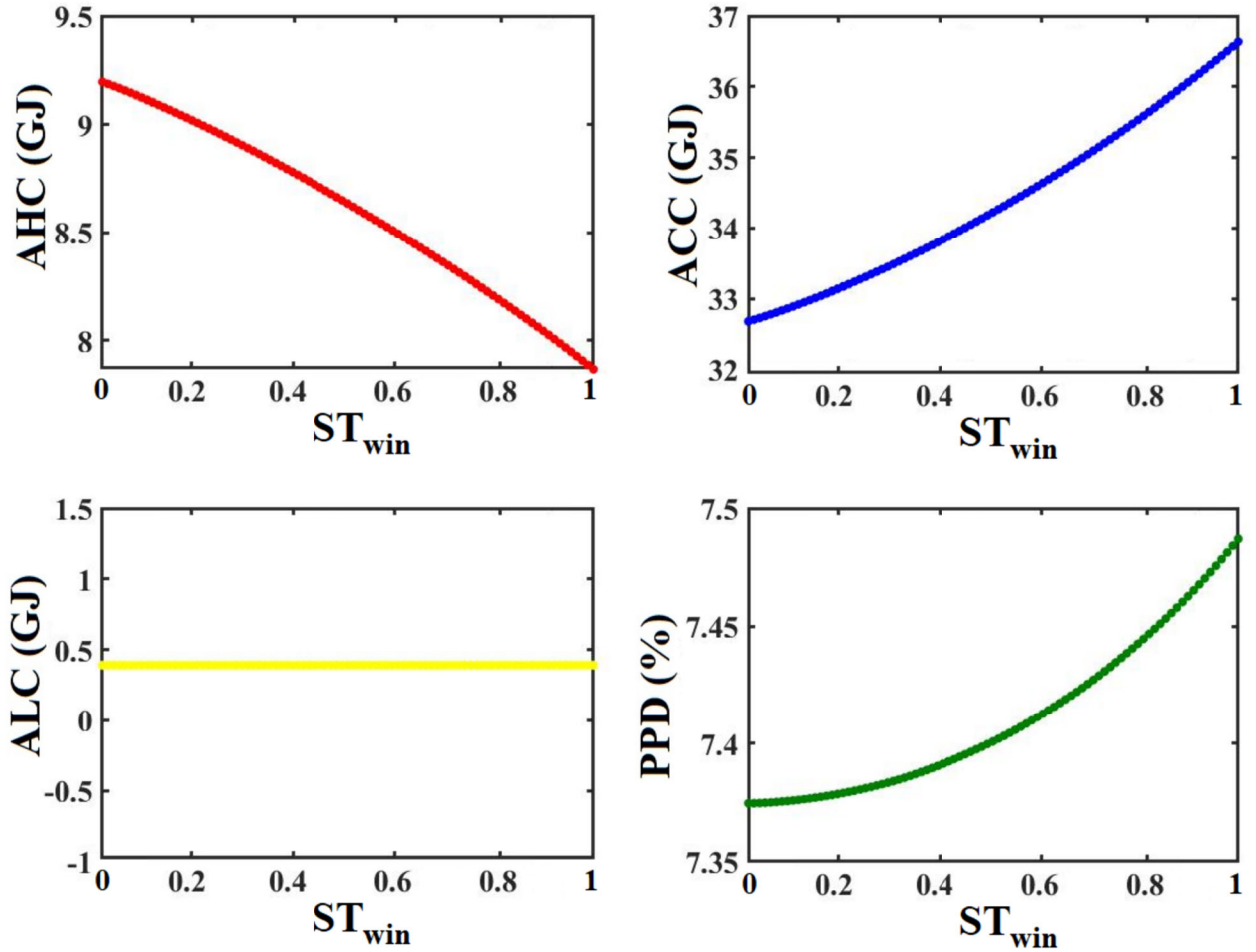

Fig. 12 Impact of ST_{win} on the AHC, ACC, ALC, and PPD

outcomes derived from Sobol's analysis, several findings were established for the building under investigation:

- Building rotation exerted the greatest influence on ALC and the least influence on PPD.
- Window-to-wall ratio had the highest impact on AHC and ALC, while it had the least impact on ACC.
- Depth of shading device had the highest influence on ALC and the least influence on PPD.
- Cooling setpoint temperature had the strongest impact on ACC and PPD, and the weakest impact on ALC and AHC.
- Heating setpoint temperature had the strongest influence on AHC and PPD, and the weakest influence on ALC and ACC.
- Solar absorptance of exterior walls had the greatest impact on AHC and the least impact on ALC.
- Thickness of exterior walls had the highest influence on AHC and the least influence on ALC.
- Solar transmittance of window glass, solar absorptance of interior walls, thickness of window glass, and thickness of gas in window did not affect ALC and had minimal influence on AHC, ACC, and PPD.
- Visible transmittance of window glass had the strongest impact on ALC and minimal impact on AHC, ACC, and PPD.
- AHC showed significant dependency on heating setpoint temperature and solar absorptance of exterior walls.
- ACC exhibited strong dependency on cooling setpoint temperature and solar absorptance of exterior walls
- ALC had substantial reliance on window-to-wall ratio and visible transmittance of window
- PPD displayed considerable dependency on heating and cooling setpoint temperatures

Additionally, upon comparing the findings from both the OAT and Sobol's analyses, it can be inferred that the sensitivity outcomes achieved through the introduced DI in OAT align closely with those of Sobol's. This correspondence arises because the DI was primarily conceived based on assessing how variations in inputs affect output variance. Without an index in OAT analysis, discerning the

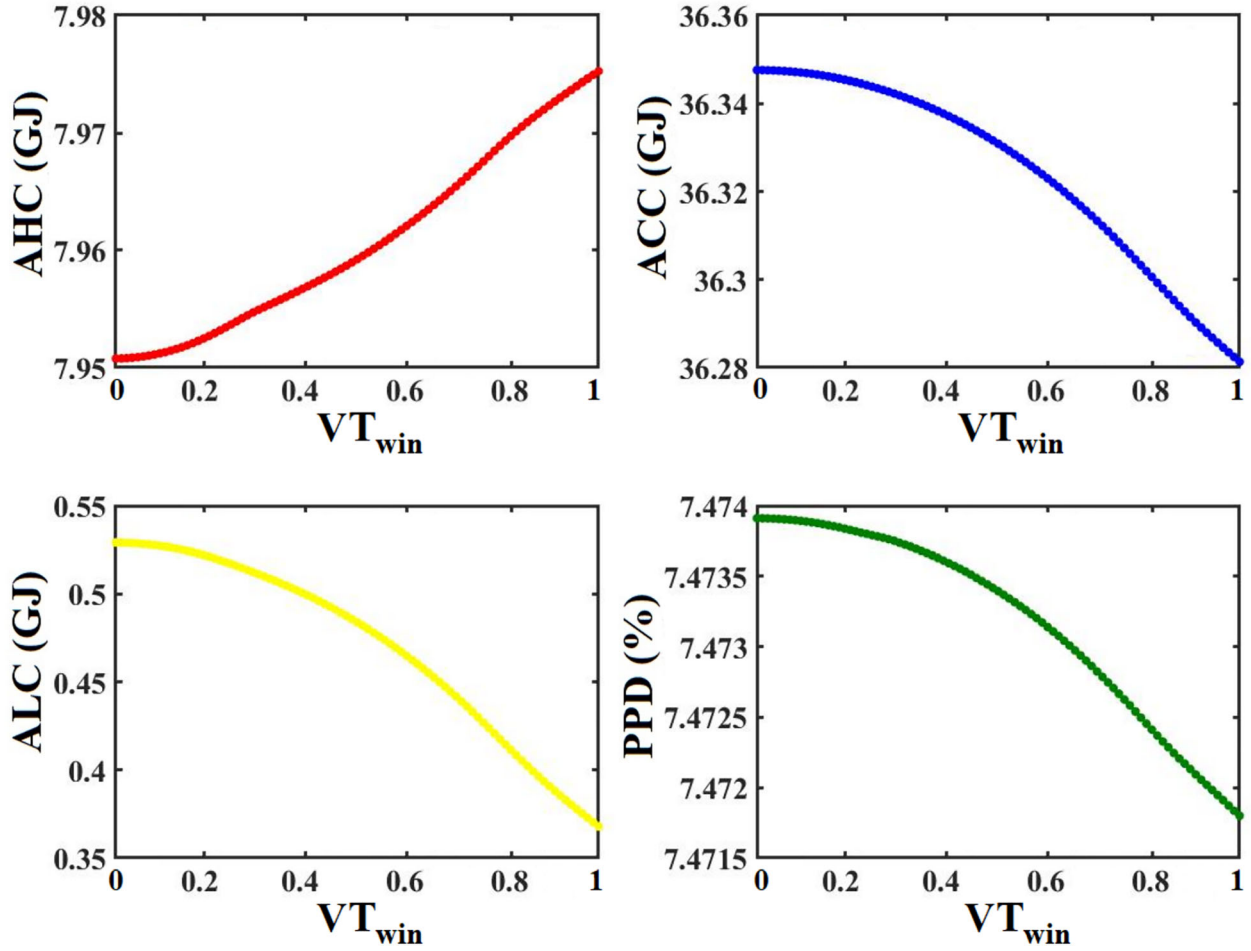

Fig. 13 Impact of VT_{win} on the AHC, ACC, ALC, and PPD

sensitivity of outputs to inputs solely through OAT graphs was impractical, primarily due to the building system's non-linear characteristics. Thus, the DI can be applied to OAT analyses of various systems to ensure robust and dependable results.

From the findings, it is evident that both OAT and Sobol's methodologies contribute distinct perspectives to SA, each characterized by unique approaches and levels of detail. The OAT approach involves systematically varying one input parameter while holding others constant, providing a straightforward means to discern the influence of individual factors on the output. This method is widely favored for its simplicity and practicality, making it suitable for initial sensitivity assessments. However, its primary drawback lies in its inability to account for interactions among variables, potentially limiting a comprehensive grasp of the system under study. Conversely, Sobol's methodology employs a more advanced approach centered on variance decomposition to assess the contribution of each input parameter to the variance of the output, encompassing both main effects and all potential interactions among variables. This approach provides a comprehensive overview of sensitivity by allowing researchers to discern not only the primary influential factors but also how these factors interact to influence the output of the system. Rooted in the mathematical framework of variance-based sensitivity analysis, Sobol's method offers a precise and detailed depiction of system behavior. However, its application demands considerably greater computational resources compared to the OAT method. Therefore, the selection between OAT and Sobol's methods should hinge upon the specific demands of the study, including the model's complexity, the number of input variables, the necessity to understand interaction effects, and the availability of computational capabilities.

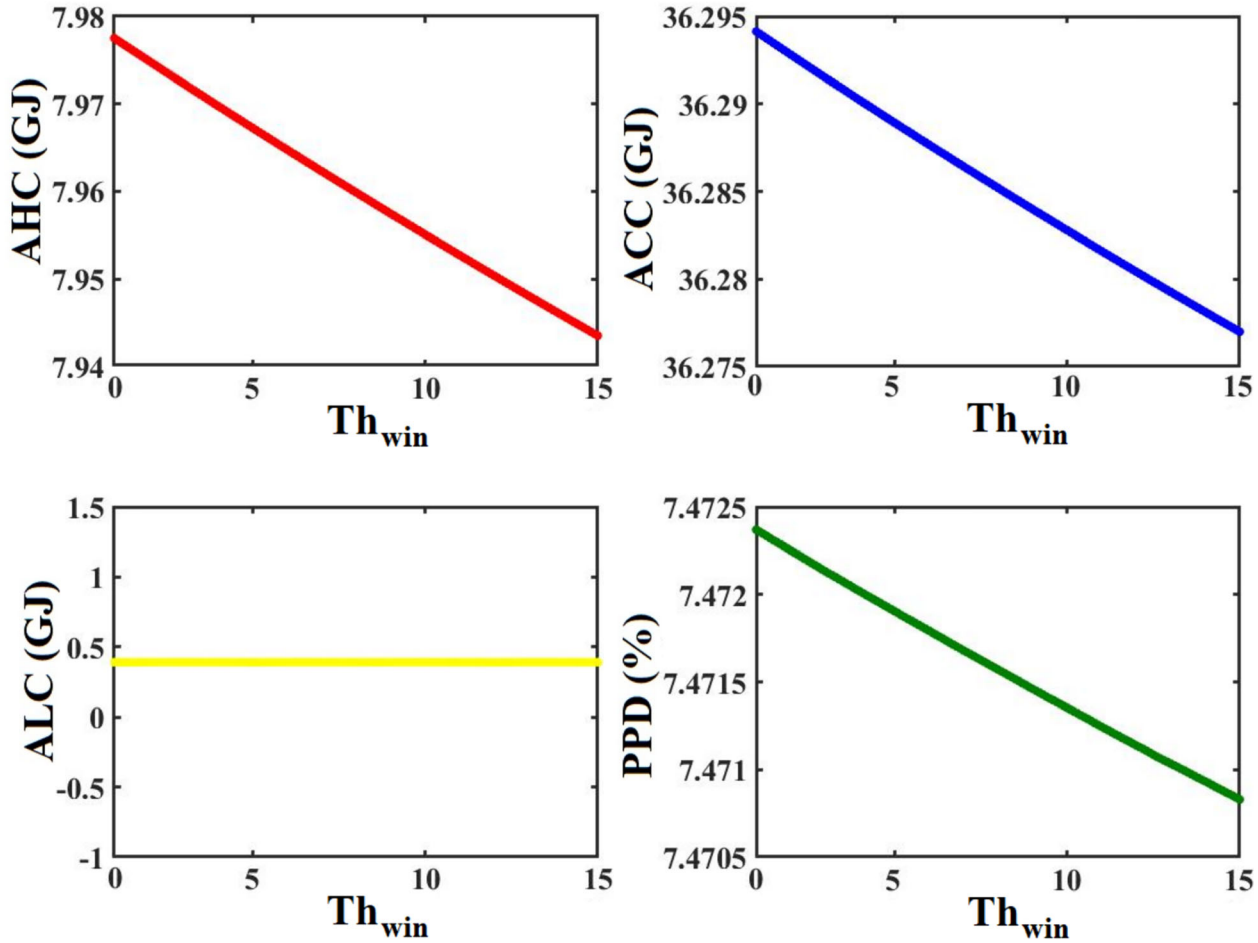

Fig. 14 Impact of Th_{win} on the AHC, ACC, ALC, and PPD

7 Conclusions

The inherent complexity of building systems underscores the importance of employing robust sensitivity analysis strategies. This study presented an innovative approach for SBSA of building performance by integrating EnergyPlus with LSA and GSA algorithms using the C++ programming language. This integration involved incorporating the capabilities and functionalities of C++ directly into EnergyPlus, enabling the direct execution of SBSA for building performance without relying on external plugins or third-party tools. To analyze the potential of the proposed method, a number of design parameters were considered as input variables. In the same respect, the SBSA process focused on building performance criteria (AHC, ACC, ALC, and PPD). The OAT analysis, employed as LSA, and Sobol's analysis, utilized as GSA, were conducted to examine how outputs respond to changes in inputs and to quantify the sensitivity of outputs to inputs. Within the LSA framework, a novel sensitivity index was proposed to precisely determine the influence of inputs on outputs. The results for the typical building under study revealed that AHC was most sensitive to the heating setpoint and the solar absorptance of exterior walls. ACC was similarly most sensitive to the cooling setpoint and solar absorptance of exterior walls. For ALC, the most influential inputs were WWR, the visible transmittance of window glass, and building orientation. In terms of PPD, cooling and heating setpoints, solar absorptance of exterior walls, and WWR were the most significant factors. Parameters such as CSPT, HSPT,SA_{IN_W}, SA_{Ex_W}, Th_{Ex_W},ST_{win}, Th_{win}, and $Th_{gas-win}$ were found to have no significant effect on ALC. Additionally, the proposed DI showed strong agreement with the S_T.

Moreover, the findings demonstrated that OAT offers a rapid and uncomplicated method to identify significant factors. It necessitates fewer model iterations, making it advantageous for computationally intensive models, and is effective in pinpointing the direct influence of each input variable on the output. Nevertheless, OAT does not consider interactions between variables. In complex systems with numerous input variables, such as building

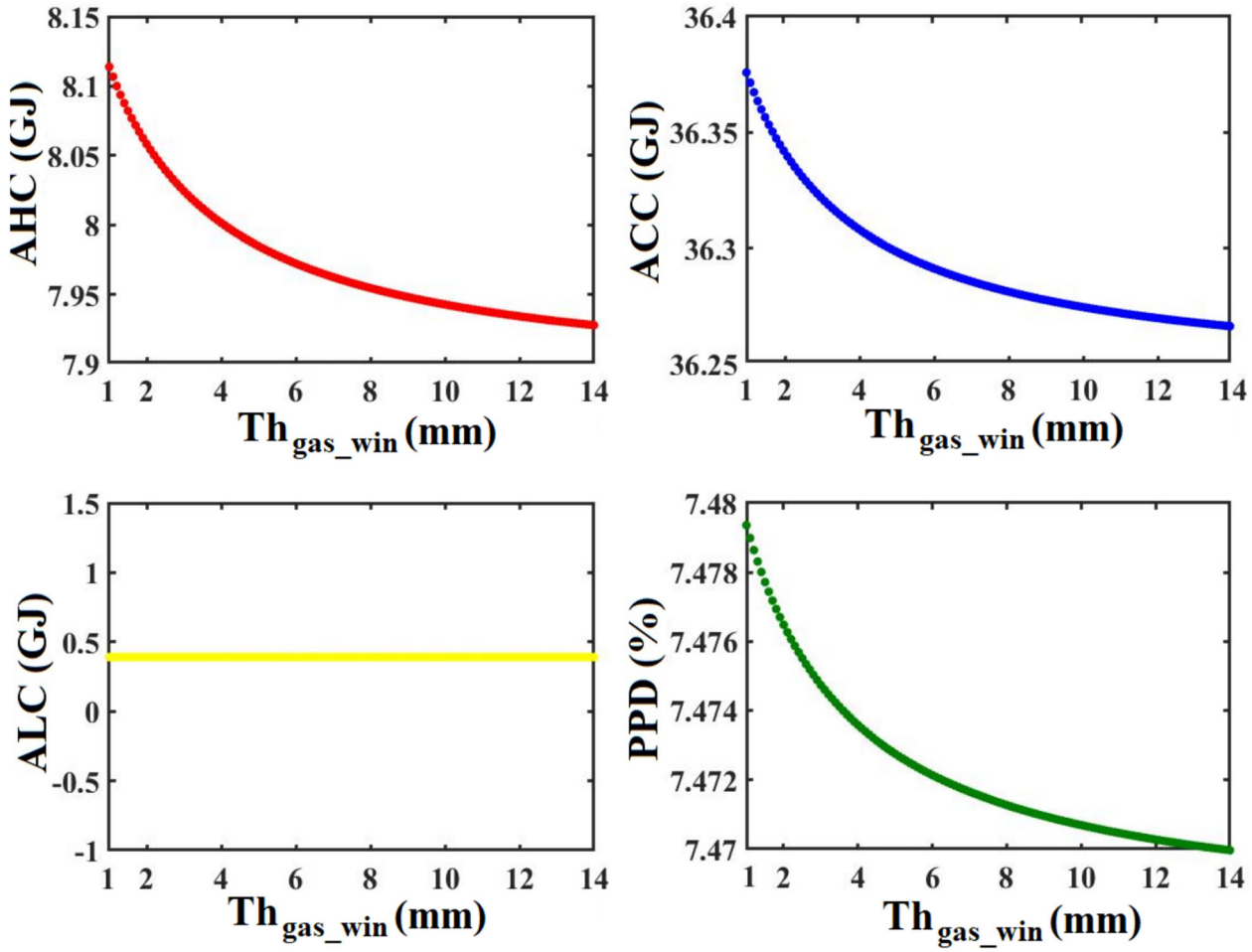

Fig. 15 Impact of $Th_{gas-win}$ on the AHC, ACC, ALC, and PPD

Table 3 Total-order SI (S_T) as per Sobol's analysis and DI as per OAT analysis

Input	AHC		ACC		ALC		PPD	
	$S_T(\%)$	$DI(\%)$	$S_T(\%)$	$DI(\%)$	$S_T(\%)$	$DI(\%)$	$S_T(\%)$	$DI(\%)$
B R	16	12	6	3	21	8	2	1
WWR	35	27	24	18	33	28	28	7
DSH	3	2	4	2	6	2	2	1
CSPT	2	1	72	54	0	0	81	64
HSPT	80	92	2	1	0	0	40	22
SA_{IN_W}	4	1	3	1	0	0	2	1
SA_{EX_W}	79	63	63	44	0	0	36	20
Th_{Ex_w}	13	10	8	6	0	0	4	2
ST_{win}	7	5	6	4	0	0	2	1
VT_{win}	2	1	2	1	25	11	3	1
Th_{win}	3	1	2	1	0	0	2	1
$Th_{gas-win}$	2	2	2	1	0	0	3	1

performance analysis, outputs often depend on interactions among multiple inputs, a factor that OAT overlooks. This limitation means that OAT may provide incomplete insights into the importance of variables or their actual impact on the system, potentially leading to misleading conclusions. In contrast, Sobol's analysis offered a detailed and intricate analysis of the sensitivity dynamics within the system, proving particularly valuable for complex models where interactions among variables heavily influence the output. However, Sobol's method entails a substantial number of model iterations, rendering it computationally demanding and resource-intensive.

These findings indicate that design specifications significantly influence building efficiency. By carefully selecting and optimizing these parameters, it is possible to achieve a building with minimal energy loss and maximal thermal comfort for residents. The introduced SBSA approach offered an effective strategy for identifying most efficient alternatives in the building design stage through the integration of advanced SA algorithms with EnergyPlus, thereby enhancing the decision-making process for building engineers by providing a broader understanding of available alternatives. Looking forward, the relevance of this research extends to building engineers and architects seeking to integrate sophisticated optimization algorithms into building design and evaluation processes. The developed framework enhances decision-making capabilities by providing a clearer overview of potential outcomes based on different design choices. This approach will ultimately facilitate a more holistic understanding of building performance, steering the future of sustainable architectural practices toward higher efficacy and precision in building design and optimization.

8 Limitations and future works

Coupling C++ with the EnergyPlus offers significant advantages in terms of flexibility and power. Our method overcomes the limitations of existing ready-made software by providing enhanced control over the selection of outputs, input parameters, algorithms, and input variables. However, this integrated approach also presents several limitations such as complexity in implementation and limited flexibility in EnergyPlus customization, which need careful consideration.

Future developments will focus on conducting multi-objective optimization to explore how different optimization variables influence specific objectives, allowing for more predictable outcomes. The method will also be applied to various building configurations across different climatic zones in Iran to assess the impact of environmental factors on building efficiency. Furthermore, expanding the scope to include other building types, such as net-zero energy buildings, and incorporating additional comfort parameters like acoustic and respiratory comfort, as well as environmental and economic impacts through life cycle assessments, will enhance the robustness of the design outputs.

Author contributions Thanks so much for everything.

Data availability No datasets were generated or analysed during the current study.

Declarations

Conflict of interest The authors declare no competing interests.

References

Almagro-Lidón M, Pérez-Carramiñana C, Galiano-Garrigós A, Emmitt S (2024) Thermal comfort in school children: testing the validity of the Fanger method for a Mediterranean climate. Build Environ 253:111305. https://doi.org/10.1016/j.buildenv.2024.111305

ANSI/ASHRAE Standard 55 (2010) Thermal environmental conditions for human occupancy. American society of heating, refrigerating and air-conditioning engineers, https://www.ashrae.org/technical-resources/bookstore/standard-55-thermal-environmental-conditions-for-human-occupancy. Accessed 23 July 2024

Arfi O, Mezaache EH, Teggar M, Laouer A (2023) Thermal analysis of a dynamic double-layer phase change material building envelope. Energy Ecology Environ 8:485–502. https://doi.org/10.1007/s40974-023-00289-2

ASHRAE climatic design conditions (2009/2013/2017/2021). http://ashrae-meteo.info/v2.0/?lat=28.9036&lng=50.8208&place=%27%27&wmo=408570&si_ip=SI&ashrae_version=2021

Baghoolizadeh M, Rostamzadeh-Renani R, Rostamzadeh-Renani M, Toghraie D (2021) A multi-objective optimization of a building's total heating and cooling loads and total costs in various climatic situations using response surface methodology. Energy Rep 7:7520–7538. https://doi.org/10.1016/j.egyr.2021.10.092

Baghoolizadeh M, Nadooshan AA, Dehkordi SAHH, Rostamzadeh-Renani M, Rostamzadeh-Renani R, Afrand M (2022) Multi-objective optimization of annual electricity consumption and annual electricity production of a residential building using photovoltaic shadings. Int J Energy Res 46:21172–21216. https://doi.org/10.1002/er.8401

Baghoolizadeh M, Rostamzadeh-Renani M, Rostamzadeh-Renani R, Toghraie D (2023a) Multi-objective optimization of Venetian blinds in office buildings to reduce electricity consumption and improve visual and thermal comfort by NSGA-II. Energy Build 278:112639. https://doi.org/10.1016/j.enbuild.2022.112639

Baghoolizadeh M, Rostamzadeh-Renani M, Hakimazari M, Rostamzadeh-Renani R (2023b) Improving CO_2 concentration, CO_2 pollutant and occupants' thermal comfort in a residential building using genetic algorithm optimization. Energy Build 291:113109. https://doi.org/10.1016/j.enbuild.2023.113109

Belyamin B, Fulazzaky MA, Roestamy M, Subarkah R (2021) Influence of cooling water flow rate and temperature on the photovoltaic panel power. Energy Ecology Environ 7:70–87. https://doi.org/10.1007/s40974-021-00223-4

Carpino C, Bruno R, Carpino V, Arcuri N (2022) Uncertainty and sensitivity analysis to moderate the risks of energy performance contracts in building renovation: a case study on an Italian social housing district. J Clean Prod 379:134637. https://doi.org/10.1016/j.jclepro.2022.134637

Chambers J, Zuberi MJS, Streicher KN, Patel MK (2021) Geospatial global sensitivity analysis of a heat energy service decarbonisation model of the building stock. Appl Energy 302:117592. https://doi.org/10.1016/j.apenergy.2021.117592

Charai M, Mezrhab A, Moga L (2022) A structural wall incorporating biosourced earth for summer thermal comfort improvement: hygrothermal characterization and building simulation using calibrated PMV-PPD model. Build Environ 212:108842. https://doi.org/10.1016/j.buildenv.2022.108842

Dara C, Hachem-Vermette C (2019) Evaluation of low-impact modular housing using energy optimization and life cycle analysis. Energy Ecology Environ 4:286–299. https://doi.org/10.1007/s40974-019-00135-4

Delgarm N, Sajadi B, Kowsary F, Delgarm S (2016a) Multi-objective optimization of the building energy performance: a simulation-based approach by means of particle swarm optimization (PSO). Appl Energy 170:293–303. https://doi.org/10.1016/j.apenergy.2016.02.141

Delgarm N, Sajadi B, Delgarm S (2016b) Multi-objective optimization of building energy performance and indoor thermal comfort: a new method using artificial bee colony (ABC). Energy Build 131:42–53. https://doi.org/10.1016/j.enbuild.2016.09.003

Delgarm N, Sajadi B, Delgarm S, Kowsary F (2016c) A novel approach for the simulation-based optimization of the buildings energy consumption using NSGA-II: case study in Iran. Energy Build 127:552–560. https://doi.org/10.1016/j.enbuild.2016.05.052

Delgarm N, Sajadi B, Azarbad Kh, Delgarm S (2018) Sensitivity analysis of building energy performance: a simulation-based approach using OFAT and variance-based sensitivity analysis methods. J Build Eng 15:181–193. https://doi.org/10.1016/j.jobe.2017.11.020

EnergyPlus V 23.1.0 (2024). https://energyplus.net/

EPA (United States Environmental Protection Agency) (2009) A guide to energy-efficient heating and cooling. https://www.energystar.gov/ia/partners/publications/pubdocs/HeatingCoolingGuide%20FINAL_9-4-09.pdf

Essa MJMA (2021) Energy management of space-heating systems and grid-connected batteries in smart homes. Energy Ecol Environ 7:1–14. https://doi.org/10.1007/s40974-021-00219-0

European Committee for Standardization (2011) Light and lighting of work places Part 1: Indoor work places (EN 12464–1).

Falk J, Angelmahr M, Schade W, Schenk-Mathes H (2021) Socio-economic impacts and challenges associated with the electrification of a remote area in rural Tanzania through a mini-grid system. Energy Ecol Environ 6:513–530. https://doi.org/10.1007/s40974-021-00216-3

Fanger PO (1970) Thermal comfort: analysis and applications in environmental engineering. McGraw-Hill, University of Michigan

Goffart J, Woloszyn M (2021) EASI RBD-FAST: an efficient method of global sensitivity analysis for present and future challenges in building performance simulation. J Build Eng 43:103129. https://doi.org/10.1016/j.jobe.2021.103129

Hai T, Delgarm N, Wang D, Karimi MH (2022) Energy, economic, and environmental (3E) examinations of the indirect-expansion solar heat pump water heater system: a simulation-oriented performance optimization and multi-objective decision-making. J Build Eng 60:105068. https://doi.org/10.1016/j.jobe.2022.105068

Hakimazari M, Baghoolizadeh M, Sajadi SM, Kheiri P, Moghaddam MY, Rostamzadeh-Renani M, Rostamzadeh-Renani R, Hamooleh MB (2024) Multi-objective optimization of daylight illuminance indicators and energy usage intensity for office space in Tehran by genetic algorithm. Energy Rep 11:3283–3306. https://doi.org/10.1016/j.egyr.2024.03.011

Hollberg A, Lichtenheld T, Klüber N, Ruth J (2017) Parametric real-time energy analysis in early design stages: a method for residential buildings in Germany. Energy Ecology Environ 3:13–23. https://doi.org/10.1007/s40974-017-0056-9

Huo H, Xu W, Li A, Chu J, Lv Y (2021) Sensitivity analysis and prediction of shading effect of external Venetian blind for nearly zero-energy buildings in China. J Build Eng 41:102401. https://doi.org/10.1016/j.jobe.2021.102401

Iran Meteorological Administration (2019–2023) Bushehr meteorological station report data processing center. https://www.irimo.ir/eng/index.php

jEPlus version 2.1 (2024). http://www.jeplus.org/wiki/doku.php?id=docs:manual_2_1

Kala Z (2021) Global sensitivity analysis based on entropy: From differential entropy to alternative measures. Entropy 23:778. https://doi.org/10.3390/e23060778

Kayalica MO, Ozozen A, Guven D, Kayakutlu G, Bayar AA (2020) Electricity consumption analysis based on Turkish household budget surveys. Energy Ecol Environ 5:444–455. https://doi.org/10.1007/s40974-020-00193-z

Li D, Jiang P, Hu C, Yan T (2023) Comparison of local and global sensitivity analysis methods and application to thermal hydraulic phenomena. Prog Nucl Energy 158:104612. https://doi.org/10.1016/j.pnucene.2023.104612

Lo Piano S, Ferretti F, Puy A, Albrecht D, Saltelli A (2021) Variance-based sensitivity analysis: the quest for better estimators and designs between explorativity and economy. Reliab Eng Syst Safety 206:107300. https://doi.org/10.1016/j.ress.2020.107300

Lotfabadi P, Hançer P (2023) Optimization of visual comfort: building openings. J Build Eng 72:106598. https://doi.org/10.1016/j.jobe.2023.106598

Maučec D, Premrov M, Leskovar VŽ (2021) Use of sensitivity analysis for a determination of dominant design parameters affecting energy efficiency of timber buildings in different climates. Energy Sustain Development/energy Sustain Dev 63:86–102. https://doi.org/10.1016/j.esd.2021.06.003

Mendes VF, Fardin W, Barreto RR, Caetano LF, Mendes JC (2022) Sensitivity analysis of coating mortars according to their specific heat, specific gravity, thermal conductivity, and thickness in contribution to the global thermal performance of buildings. Sustain Mater Technol 31:e00381. https://doi.org/10.1016/j.susmat.2021.e00381

Nasouri M, Delgarm N (2022a) Bushehr Nuclear Power Plants (BNPPs) and the perspective of sustainable energy development in Iran. Prog Nucl Energy 147:104179. https://doi.org/10.1016/j.pnucene.2022.104179

Nasouri M, Delgarm N (2022b) Numerical modeming, energy-exergy analyses, and multi-objective programming of the solar-assisted heat pump system using genetic algorithm coupled with the multi-criteria decision analysis. Arab J Sci Eng 48:3537–3557. https://doi.org/10.1007/s13369-022-07151-3

Nasouri M, Delgarm N (2023) Efficiency-based Pareto optimization of building energy consumption and thermal comfort: a case study of a residential building in Bushehr. Iran J Therm Sci/J Therm Sci 33:1037–1054. https://doi.org/10.1007/s11630-023-1933-5

Nasouri M, Bidhendi GN, Amiri MJ, Delgarm N, Delgarm S, Azarbad Kh (2021) Performance-based Pareto optimization and multi-attribute decision making of an actual indirect-expansion solar-

assisted heat pump system. J Build Eng 42:103053. https://doi.org/10.1016/j.jobe.2021.103053

Pang Z, O'Neill Z, Li Y, Niu F (2020) The role of sensitivity analysis in the building performance analysis: a critical review. Energy Build 209:109659. https://doi.org/10.1016/j.enbuild.2019.109659

Pianosi F, Wagener T (2015) A simple and efficient method for global sensitivity analysis based on cumulative distribution functions. Environ Model Softw 67:1–11. https://doi.org/10.1016/j.envsoft.2015.01.004

Ramin H, Hanafizadeh P, Akhavan-Behabadi MA (2015) Determination of optimum insulation thickness in different wall orientations and locations in Iran. Adv Build Energy Res 10:149–171. https://doi.org/10.1080/17512549.2015.1079239

Rentzeperis F, Wallace D (2022) Local and global sensitivity analysis of spheroid and xenograft models of the acid-mediated development of tumor malignancy. Appl Math Model 109:629–650. https://doi.org/10.1016/j.apm.2022.05.006

Saha SP, Ghosh S, Mazumdar D, Ghosh S, Ghosh D, Sarkar MM, Roy S (2023) Valorization of banana peel into α-amylase using one factor at a time (OFAT) assisted artificial neural network (ANN) and its partial purification, characterization, and kinetics study. Food Biosci 53:102533. https://doi.org/10.1016/j.fbio.2023.102533

Salilih EM, Abu-Hamdeh NH, Khoshaim A, Almasri RA, Sajadi SM, Karimipour A (2022) Thermal systems energy optimization employing two independent circuits of double vertical ground U-tube with PCM as the backfill material for building. J Build Eng 56:104752. https://doi.org/10.1016/j.jobe.2022.104752

Saltelli A, Ratto M, Andres T, Campolongo F, Cariboni J, Gatelli D, Saisana M, Tarantola S (2007) Global sensitivity analysis the primer. John Wiley & Sons, England

Saltelli A, Annoni P, Azzini I, Campolongo F, Ratto M, Tarantola S (2010) Variance based sensitivity analysis of model output. Design and estimator for the total sensitivity index. Comput Phys Commun 181:259–270. https://doi.org/10.1016/j.cpc.2009.09.018

Shen Y, Yarnold M (2021) A novel sensitivity analysis of commercial building hybrid energy-structure performance. J Build Eng 43:102808. https://doi.org/10.1016/j.jobe.2021.102808

Shin M, Haberl JS (2022) A procedure for automating thermal zoning for building energy simulation. J Build Eng 46:103780. https://doi.org/10.1016/j.jobe.2021.103780

SketchUp V 2023.0.1 (2024). https://www.sketchup.com/

Vuillod B, Montemurro M, Panettieri E, Hallo L (2023) A comparison between Sobol's indices and Shapley's effect for global sensitivity analysis of systems with independent input variables. Reliab Eng Syst Saf 234:109177. https://doi.org/10.1016/j.ress.2023.109177

Wang H, Lin C, Hu Y, Zhang X, Han J, Cheng Y (2023) Study on indoor adaptive thermal comfort evaluation method for buildings integrated with semi-transparent photovoltaic window. Build Environ 228:109834. https://doi.org/10.1016/j.buildenv.2022.109834

Xu B, Wang S, Xia H, Zhu Z, Chen X (2023) A global sensitivity analysis method for safety influencing factors of RCC dams based on ISSA-ELM-Sobol. Structures 51:288–302. https://doi.org/10.1016/j.istruc.2023.03.027

Yang S, Fiorito F, Prasad D, Sproul A, Cannavale A (2021) A sensitivity analysis of design parameters of BIPV/T-DSF in relation to building energy and thermal comfort performances. J Build Eng 41:102426. https://doi.org/10.1016/j.jobe.2021.102426

Yip S, Athienitis AK, Lee B (2021) Early stage design for an institutional net zero energy archetype building. Part 1: methodology, form and sensitivity analysis. Sol Energy 224:516–530. https://doi.org/10.1016/j.solener.2021.05.091

Yu S, Hao S, Mu J, Tian D (2022) Optimization of wall thickness based on a comprehensive evaluation index of thermal mass and insulation. Sustainability 14:1143. https://doi.org/10.3390/su14031143

Zamanipour B, Ghadaksaz H, Keppo I, Saboohi Y (2023) Electricity supply and demand dynamics in Iran considering climate change-induced stresses. Energy 263:126118. https://doi.org/10.1016/j.energy.2022.126118

Zeferina V, Wood FR, Edwards R, Tian W (2021) Sensitivity analysis of cooling demand applied to a large office building. Energy Build 235:110703. https://doi.org/10.1016/j.enbuild.2020.110703

Zhang X, Trame M, Lesko L, Schmidt S (2015) SOBOL Sensitivity Analysis: a tool to guide the development and evaluation of systems pharmacology models. CPT Pharmacomet Syst Pharmacol 4:69–79. https://doi.org/10.1002/psp4.6

Zhang Y, Zhang X, Huang P, Sun Y (2020) Global sensitivity analysis for key parameters identification of net-zero energy buildings for grid interaction optimization. Appl Energy 279:115820. https://doi.org/10.1016/j.apenergy.2020.115820

Zheng P, Wu H, Liu Y, Ding Y, Yang L (2022) Thermal comfort in temporary buildings: a review. Build Environ 221:109262. https://doi.org/10.1016/j.buildenv.2022.109262